

Geomorphologic Assessment of the Rio Grande San Acacia Reach

Final Report



United States Department of the Interior
Bureau of Reclamation
Albuquerque Area Office
555 Broadway NE Suite 100
Albuquerque, NM 87102-2352

Acknowledgements:

Field Data Collection Crew:

Travis Bauer, Tamara Massong, Marvin Murphy, Mark Nemeth, Robert Padilla, and Kristi-Irene Smith. Contractors: FLO Engineering, and Tetra Tech ISG.

Aerial Photography:

Jan Oliver. Contractors: Koogle and Pouls Engineering, Inc.

Figure Preparation:

Travis Bauer, Cord Everetts, Tamara Massong, Mark Nemeth, and Kimberly Shelton.

Data Analysis and Report Writing:

Travis Bauer, Tamara Massong, and Mark Nemeth.

Report Reviews:

Drew Baird, Karl Martin, Robert Padilla, Michael Porter, and Kristi-Irene Smith.

Funding:

USBR-Albuquerque Area Office River Maintenance Project.

TABLE OF CONTENTS

LIST OF FIGURES	4
LIST OF TABLES	6
SUMMARY	8
1.0 INTRODUCTION/PURPOSE OF STUDY.....	11
2.0 WATERSHED AND REACH INFLUENCES.....	13
2.1 Watershed and Local Geology.....	13
2.2 Human Influences	14
3.0 HISTORY OF PRECIPITATION, FLOWS AND SEDIMENT	16
3.1 Precipitation History	16
3.2 Gaged Stream Flow and Sediment History.....	18
3.3 Local Supplies of Gravel and Sand.....	21
4.0 RIVER CHARACTERISTICS.....	26
4.1 Terraced Surfaces.....	27
4.1.1 Terrace 1 and 2.....	29
4.1.2 Terrace 3 and 4.....	29
4.1.3 Terrace 5 and 6.....	31
4.1.4 Terrace Summary.....	31
4.2 Channel Forming Flow	32
4.3 Sub-Reach Designation and Channel Classification.....	34
4.3.1 Reach and Sub-Reach Descriptions	34
4.3.2 Rosgen’s Description Based Classification Model.....	41
4.3.3 Empirical Classification Models.....	42
4.4 Current and Historic Cross Section Dimensions	42
4.4.1 Average Reach Conditions	43
4.4.2 Sub-Reach 1 Conditions	46
4.4.3 Sub-Reach 2 Conditions	48
4.4.4 Sub-Reach 3 Conditions	50
4.4.5 Sub-Reach 4 Conditions	52
4.5 Bed Material - Sediment Characteristics	53
4.6 Sand Load from Upstream Sources	57
4.7 Sand Load from the River Channel	58
4.8 Sediment Routing.....	58
5.0 EQUILIBRIUM SLOPE AND FUTURE CONDITIONS ASSESSMENT	64
5.1 Equilibrium Slope and Width Analysis	64
5.1.1 Historical Slopes	64
5.1.2 Equilibrium Bed Slope based on Sediment Size.....	64
5.1.3 Estimated Equilibrium Slope and Width based on Sediment Supply.....	66
5.1.4 Summary of Equilibrium Slopes and Widths from Sediment Transport Models	66
5.2 Stable Sediment Sizes	67
5.3 Future Conditions - No Action Scenario	68
5.3.1 Future Conditions of Sub-Reach 1.....	68
5.3.2 Future Conditions of Sub-Reach 2.....	68

5.3.3 Future Conditions of Sub-Reach 3.....	69
5.3.4 Future Conditions of Sub-Reach 4.....	70
5.3.5 Potential Levee Breach Locations	71
5.3.5 Summary of Future Conditions.....	73
6.0 CONCLUSIONS	74
7.0 LITERATURE CITED	75

LIST OF FIGURES

- Figure 1 Location map displaying San Acacia reach location and weather station locations.
- Figure 2 Faulted surface (fault #1 is upstream of fault #4) along the Rio Grande, San Acacia Reach.
- Figure 3 Average Monthly Discharges – USGS Rio Grande gage at the San Acacia Floodway
- Figure 4 Average Monthly Suspended Sediment – USGS Rio Grande gage at the San Acacia Floodway.
- Figure 5 Cumulative Snowfall Records in Southern Colorado.
- Figure 6 Yearly Total Precipitation at Socorro, NM and Bernardo, NM.
- Figure 7 Annual discharge given in year discharge and cumulative – USGS Rio Grande gage at San Acacia, NM.
- Figure 8 Annual sediment load given in year discharge and cumulative – USGS Rio Grande gage at San Acacia, NM.
- Figure 9 Cumulative suspended sediment and discharge – USGS Rio Grande gages at San Acacia, NM and San Marcial, NM.
- Figure 10 Historic Well Logs in the San Acacia Reach.
- Figure 11a Sub-Reach location map showing Sub-reaches 1, 2 and the northern portion of sub-reach 3, Rio Grande – San Acacia Reach.
- Figure 11b Sub-Reach location map showing the southern portion of sub-reach 3 and sub-reach 4, Rio Grande – San Acacia Reach.
- Figure 12 Terraced surfaces along the Rio Grande – San Acacia Reach.
- Figure 13 Stratigraphic columns of two terraces along the Rio Grande - San Acacia Reach.
- Figure 14 Flood frequency curve, Rio Grande – San Acacia Reach.
- Figure 15a Historic trends in channel location, Rio Grande – San Acacia Reach: 1918, 1935, 1949 channel locations.
- Figure 15b Historic trends in channel location, Rio Grande – San Acacia Reach: 1918, 1962, 1972 channel locations.
- Figure 15c Historic trends in channel location, Rio Grande – San Acacia Reach: 1918, 1985, 1992 and 2002 channel locations.
- Figure 16 Historic trends in channel Sinuosity, Rio Grande – San Acacia Reach.
- Figure 17 Historic channel width, Rio Grande – San Acacia Reach.
- Figure 18 Channel widths and overbanking since 1962, Rio Grande – San Acacia reach.
- Figure 19 Bed Material Measurements at the USGS Rio Grande gage, San Acacia.
- Figure 20 Monthly variability in grain sizes at the USGS Rio Grande gage, San Acacia.
- Figure 21 Particle size distribution of gravel layer, Rio Grande – San Acacia Reach.
- Figure 22 Estimated sand load results from the modified Einstein procedure, Rio Grande gage at San Acacia.
- Figure 23 Sediment Transport Zone Locations, Rio Grande – San Acacia Reach

- Figure 24 USGS Rio Grande gage (at San Acacia) discharge data for a wet year (1994) and the corresponding sediment discharge.
- Figure 25 USGS Rio Grande gage (at San Acacia) discharge data for a dry year (1996) and the corresponding sediment discharge.
- Figure 26 USGS Rio Grande gage (at San Acacia) discharge data for a 5-year period (1990-1995) and the corresponding sediment discharge.
- Figure 27 Future elevation conditions of Sub-Reach 4, Rio Grande – San Acacia Reach.
- Figure 28 Three USBR river maintenance priority sites with levee erosion concerns, plus one site of estimated future levee erosion (the downstream most highlighted section), Rio Grande; San Acacia Reach.

LIST OF TABLES

Table 1	Samples of bed material from tributaries within or near the San Acacia Reach.
Table 2	Summary information for the San Acacia Reach terraces.
Table 3	Effective discharge calculations, USGS Rio Grande gage at San Acacia.
Table 4	Sub-reach description and lengths.
Table 5	Summary of active channel widths in feet, by year, as measured from the distance between riparian vegetation on historic aerial photos, San Acacia Reach.
Table 6	Classification assigned to each sub-reach by each model.
Table 7	Summary of reach average values for the San Acacia Reach as estimated from riparian boundaries on the historic photographs, and by the HEC-RAS and STARS models.
Table 8	Summary of sub-reach 1 average values for the San Acacia Reach as estimated from riparian boundaries on the historic photographs, and by the HEC-RAS and STARS models.
Table 9	Summary of sub-reach 2 average values for the San Acacia Reach as estimated from riparian boundaries on the historic photographs, and by the HEC-RAS and STARS models.
Table 10	Summary of sub-reach 3 average values for the San Acacia Reach as estimated from riparian boundaries on the historic photographs, and by the HEC-RAS and STARS models.
Table 11	Summary of sub-reach 4 average values for the San Acacia Reach as estimated from riparian boundaries on the historic photographs, and by the HEC-RAS and STARS models.
Table 12	Grain sizes (d_{84}) throughout the San Acacia Reach.
Table 13	Summary of gravel layer characteristics by sub-reach.
Table 14	Volume of sediment removed by bed lowering (degradation) for each sub-reach in the San Acacia Reach, as determined by cross section comparisons.
Table 15	Summary of Sediment Transport Zones, San Acacia Reach.
Table 16	Current Conditions of Channel Parameters for each Transport Zone, San Acacia Reach.
Table 17	Summary of average water surface slopes, San Acacia Reach (1962-1999).
Table 18	Computed stable slopes for sand and gravel sized sediment for San Acacia Reach.
Table 19	Computed stable width and EG slopes for the current channel conditions and sediment supply for flows of 5,000 cfs: San Acacia Reach.

- Table 20 Grain sizes present, estimated sizes of grain mobile during a 5,000 cfs discharge and the specific discharge required to mobilize the current grains on the channel bed in the San Acacia Reach
- Table 21 Average future conditions for sub-reach 3 based on a slightly meandering, gravel bedded channel, San Acacia Reach.

SUMMARY

A geomorphic study of the Rio Grande between San Acacia Diversion Dam and Escondida Bridge (San Acacia Reach) found that physical channel features, sediment discharge, sediment size and channel morphology have changed significantly from historic conditions, and that these changes will continue to evolve in the future. The total length of the reach is approximately 10.5 miles (17 km).

A series of storage reservoirs built in the 1950's-1970's, upstream from this study site, control spring runoff flows and decrease the sediment load. As precipitation generally increased in the 1980's, annual spring runoff volume also increased, however, any flows approaching floodstage were retained in the reservoirs to be released at slower rates throughout the subsequent months. The current volume of suspended sediment at San Acacia (1980-1999) has decreased to approximately 20% of sediment levels measured prior to the closure of Cochiti Reservoir in 1975.

Although major channel modifications in the San Acacia area began in the 1930's with the building of the diversion dam and a railroad line along the west (right) side of the river channel, significant modifications were made to the floodway in the 1950's and 1960's with the building of the Low Flow Conveyance channel (LFCC). Modifications to the floodway during the 1950's and 1960's included channel straightening, narrowing through re-alignment and jetty jacks, riparian vegetation management, and riverbed grading/in-channel debris removal. A levee on the west side of the river that extends the entire length of the reach was created from the LFCC channel spoils.

The San Acacia Reach is divided into 4 sections or sub-reaches with sub-reach 1 starting at the San Acacia diversion dam and sub-reach 4 ending at Escondida Bridge. Sub-reach 1 (1.3 mi or 2 km) is a narrow, straight, tightly confined, single threaded channel. The second sub-reach (2.2 mi or 3.5 km) is also narrow and single threaded, but also exhibits a slightly meandering morphology where point bars have developed on the inside of the meander bends. The third sub-reach (5.7 mi or 9.2 km) has a relatively wide channel and is dominantly a braided morphology at low flows. Sub-reach 4 (1.4 mi or 2.1 km) is similar to sub-reach 1, in that it is a straight, single threaded channel which is confined by terraces and levees.

Although channel straightness has not changed significantly since 1918, channel pattern has. In 1918, almost the entire reach was wide and braided at low flows. Sub-reaches 1, 2 and 4 were modified significantly during the channelization period of the 1950's; sub-reaches 1 and 4 are now very narrow straight channels. Sub-reach 2 is less confined than sub-reaches 1 and 4, and is meandering slightly. Sub-reach 3 was modified less than the other reaches and has maintained a wider channel, but it has begun to convert to a meandering form as found in sub-reach 2. Along with these larger-scale pattern changes, the width of the channel has decreased 60% since 1918, depth has doubled since 1962 and the channel bed elevation has decreased from 8-13 feet.

The channel forming flow was determined using three methods: effective flow, recurrence interval analysis, and bankfull measurements. Effective discharge calculations indicate that the most sand is transported at 2,800-3,200 cfs. The recurrence interval analysis for wet periods (1979-1997) and for dry periods (1959-1979), indicated that a flow of 5,000 cfs had a recurrence of 1.5 and 2.5 years respectively. Bankfull estimates found that a flow with a mean daily discharge of approximately 5,000 cfs just filled the active channel. Since the channel has a bimodal sediment size, the channel forming flow used in this assessment is 5,000 cfs, for the general channel form and the gravel bed, while a flow of 3,000 is used for channel form relating to the sand sized sediment.

A series of terraces define two distinct periods of degradation (i.e., channel bed lowering due to limited sediment supply): 1918-1949 and 1985-1995. Terraces from the first period of degradation are 8-12 feet above the current channel, while the second set of terraces are 3-6 feet. Since the 1962 survey data (the earliest survey data collected), the channel bed has decreased in elevation approximately 13 feet near the dam, and 8 feet near Escondida Bridge. Along with the levee, the terraces increase the extent of channel confinement.

Consistent with degradation, the size of sediment lining the channel bed has also increased. In approximately 1988, gravel sized sediment was sampled at the San Acacia gage, and appears to mark the transition of sub-reach 1 from a historically sand bedded river to a gravel bedded river. Although the channel bed and its physical characteristics are now controlled by the gravel sized sediment, sand sized particles still cover portions of the bed. Gravel is found in all sub-reaches, however, a continuous layer has only formed in sub-reaches 1, 2 and part of 3. Sediment transport models and field observations indicate that sand sized sediment is transported at most flow regimes (>300 cfs), while the gravel is mostly transported at channel forming flows (>5,000 cfs). At these channel forming flows, transport models show that the sand is rapidly transported out of the reach, in fact, the average spring runoff alone is estimated to fully scour the current deposits of sand found in sub-reaches 1 and 2.

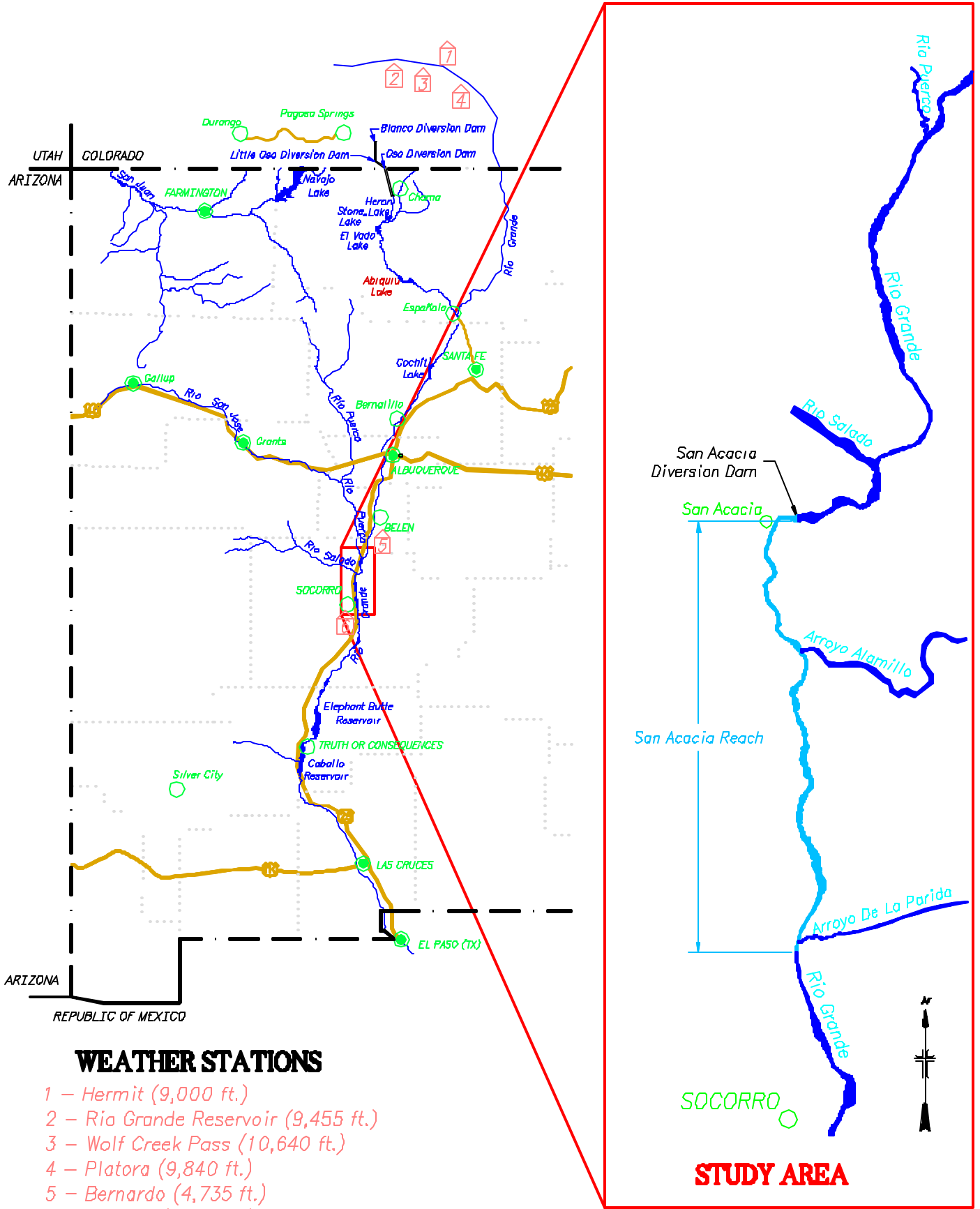
Estimated future condition analyses indicate that sub-reaches 1 and 2 will probably not change significantly in the near future with the current supply of sediment and flows, however sub-reaches 3 and 4 will likely continue to evolve. The channel of sub-reach 3 appears to be in the most transient state of the sub-reaches. The upstream section of sub-reach 3 is currently converting to a meandering channel pattern similar to sub-reach 2, grain size on the channel bed is coarsening to gravel, and the bed continues to degrade. Sub-reach 3 will likely evolve to a meandering channel pattern that will produce an even narrower, deeper and longer channel with a decreasing slope. With this evolution (sub-reach 3), the timing of sediment transport will change from the current year-round transport at low to moderate flow towards sediment transport of gravel sized sediment during channel forming flows. Other than channel bed elevation, channel features in sub-reach 4 have changed very little since it was channelized in the 1950's. The recent protrusion of Arroyo de la Parida's sediment fan into the Rio Grande's channel, near the end of this sub-reach is creating a natural grade control feature in the main channel. Once the grade control feature is fully established (estimated within 2 years), modest aggradation is

expected upstream throughout sub-reach 4, thus breaking the degradation pattern and establishing a more stable channel bed elevation.

1.0 INTRODUCTION/PURPOSE OF STUDY

Since both wildlife and humans depend on the Rio Grande as a source of water, interest in the evolution of this river is extensive. Historically, human needs have dominated water management decisions along the Rio Grande, but recent listing of the Rio Grande silvery minnow and the southwestern willow flycatcher as endangered species has heightened the need to include wildlife needs in resource management decisions. The challenge for decision makers today is to produce management plans that are beneficial to both humans and wildlife. In order to make these decisions, they need to know how the Rio Grande has evolved and how it will continue to evolve with current management practices.

The San Acacia Reach (Figure 1) of the Rio Grande extends from the San Acacia diversion dam downstream to the bridge crossing the Rio Grande near Escondida (10.5 miles/17 km). Photos and maps dating back to the early 1900's provide a historic basis for comparisons of channel form and general characteristics. Channel surveys date from 1962 to 1999. The purpose of the study is to determine historic channel conditions of both the river and its floodplain, determine current conditions, understand how and why the channel evolved from the historic conditions, and predict future channel morphology under the current management regime.



WEATHER STATIONS

- 1 – Hermit (9,000 ft.)
- 2 – Rio Grande Reservoir (9,455 ft.)
- 3 – Wolf Creek Pass (10,640 ft.)
- 4 – Platora (9,840 ft.)
- 5 – Bernardo (4,735 ft.)
- 6 – Socorro (4,485 ft.)

Figure 1: Location map displaying San Acacia reach location and weather station locations.

2.0 WATERSHED AND REACH INFLUENCES

2.1 Watershed and Local Geology

Two large scale geologic processes influence the geomorphic evolution of the middle Rio Grande valley: extensional faulting parallel to the valley, or rifting (Chapin, 1988), and volcanism both within the watershed producing rhyolitic through andesitic rocks (Morgan et al, 1986) and along the mainstem river producing andesitic through basaltic rocks (R. M. Chamberlin, and W. C. McIntosh, N.M. Bureau of Mines and Mineral Resources, N.M. Geochronology Research Lab, unpub. data, written commun., 2000; and Morgan et al, 1986). Extensional faulting, associated with the Rio Grande rifting has created a north-south extending valley, in which the Rio Grande valley is subsiding relative to the mountains which are uplifting. This rifting valley is partially filled by debris (sediment) originating from the mountains, volcanism and sediments transported by the Rio Grande which are estimated to be up to 5,000 feet thick (Hawley, 1978) in the Socorro area. Lava flows also fill this valley, such as the andesite at San Acacia (R. M. Chamberlin, and W. C. McIntosh, N.M. Bureau of Mines and Mineral Resources, N.M. Geochronology Research Lab, unpub. data, written commun., 2000).

Two local geologic features/processes greatly influence the San Acacia reach: the andesitic volcano at San Acacia, and a magma body beneath the surface in the San Acacia area, also known as the Socorro Magma Body. The andesitic lava located at San Acacia (R. M. Chamberlin, and W. C. McIntosh, N.M. Bureau of Mines and Mineral Resources, N.M. Geochronology Research Lab, unpub. data, written com., 2000) is present on both sides of the channel, creating a naturally narrow or confined section of the Rio Grande. Argon-Argon dating of these rocks indicate that the magma eruption occurred approximately 4.87 ± 0.04 million years ago (R. M. Chamberlin, and W. C. McIntosh, N.M. Bureau of Mines and Mineral Resources, N.M. Geochronology Research Lab, unpub. data, written com., 2000). Landslides in this volcanic material originate from both sides of the river, which may have further constricted the Rio Grande. These landslides also provide large bed material which is not readily transported by river processes. Although no dates have been established for the landslides, earlier photographs from 1906, clearly show that the west-side landslide had already occurred (Scurlock, 1998). A strath terrace (a terrace in which river sediments overlie an eroded bedrock surface) is located immediately downstream of the landslide deposits. Although this terrace has not been dated either, historic photos indicate that it was also formed prior to the 1900's.

The other main geologic influence on this reach is differential uplift associated with the rise of a magma body (Sanford et al., 1973; Sanford et al., 1977; Brown et al., 1979; and Larsen and Reilinger, 1983). The center of uplift, located approximately 2 miles (3 km) upstream of the study reach (Larsen and Reilinger, 1983; and Ouchi, 1983), was rising at an estimated rate of 1.8 ± 0.5 mm/yr between 1951-1980. Since uplift rates are not uniform (the center of the magma body is rising faster than the flanks), surface slopes downstream of the center of uplift are increasing, while slopes upstream from the center are decreasing. Also, extensional faults have been found in two fluvial terraces that are both less than 50 years old downstream of San Acacia (Figure 2): the visible fault lines appear generally consistent with extensional faulting and hence, surface uplift from a magma body.

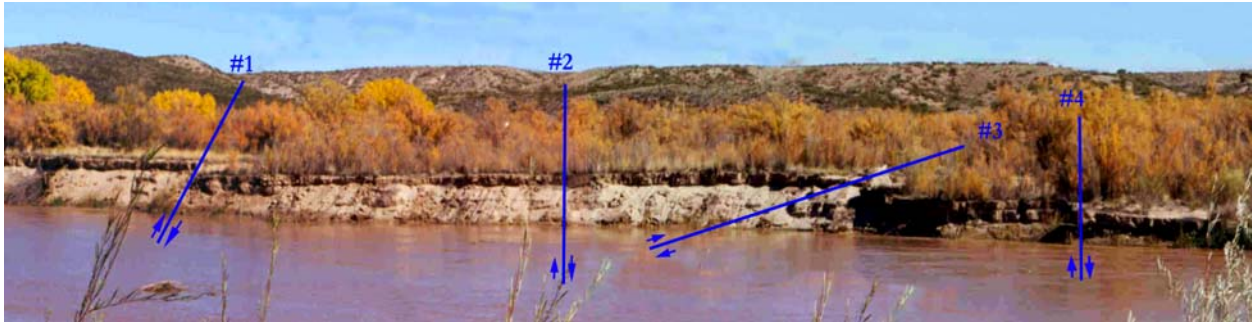


Figure 2: Faulted surface (fault #1 is upstream of fault #4) along the Rio Grande, San Acacia Reach.

2.2 Human Influences

The Middle Rio Grande valley is one of the oldest agricultural areas in the United States, reaching a peak of irrigated lands in 1880 at 124,000 acres (Lagasse 1980). Due to the progressing decrease in irrigated lands after 1880 and flooding in the early part of the century, the U.S. Congress authorized the Rio Grande Reclamation Project in 1905 and later the Rio Grande Comprehensive Plan, authorized in the Flood Control Acts of 1948 and 1950. These acts authorized the rehabilitation of the Middle Rio Grande Conservancy District, river channel rectification, maintenance, and sediment/flood retention dams to be built along the Rio Grande and its tributaries. The purpose of these acts was to reduce and reverse river aggradation, increase agricultural land use, protect important river side facilities, provide valley drainage along the Rio Grande and increase water delivery to Elephant Butte Reservoir under the Rio Grande Compact. Most of the levees, riverside drainage canals and small diversions dams were built in the 1930's and are administered by the Middle Rio Grande Conservancy District. The sediment and water storage dams upstream of San Acacia were built between 1953 (Jemez Canyon Dam) and 1973 (Cochiti Dam), including the Gallesteo dam. During the same period, Kellner jetty jack systems and stream-side drainage canals were rehabilitated along the Rio Grande. Along with the levees and stream-side canals, this period also saw the re-alignment and straightening of the Rio Grande floodway: an activity which still affects floodway morphology today.

Engineered structures/features in the study reach consist of an irrigation and water delivery diversion dam, levees, riverside railroad line, Kellner jetty jack lines and a bridge crossing. San Acacia diversion dam was built in 1935 and currently diverts water into the Socorro Main diversion canal and the Low Flow Conveyance Channel (LFCC). Located between two andesitic outcrops, the diversion dam is in a naturally narrow section of the Rio Grande. The river channel bed downstream of the dam is lined by boulder-sized sediment, rock debris from the andesite, and rip-rap placed after construction of the dam. The persistently narrow channel downstream of the dam is confined for about 0.5 miles by the Atchison Topeka & Santa Fe Railroad line. The remaining 10 miles of the reach is confined by abandoned river surfaces and the levee. The levee was originally constructed from the LFCC spoils in the mid-1950's (Chris Gorbach, USBR, pers. comm., 1999) and is located on the west (right) side of the river, and extends past the Escondida Bridge. Smaller, unconnected spoil piles that act as local

levees are located throughout the reach, mostly on the right bank. These spoils appear to originate from realignment efforts of the floodway during the building of the LFCC. The Kellner jetty jack lines were constructed in approximately the 1950's, and are located on the historic floodplain along the levee. These jetties were originally constructed to protect the levee from bank erosion and channel avulsions. Nearly all the jetty jacks are still in place. The Escondida bridge was built prior to the 1950's in a naturally narrow section of the Rio Grande; the Rio Grande channel/floodplain is impinged by the distinct debris fan from the Magdalena Mountains to the west and ancient river sediments to the east. After these large-scale channel modifications were completed, riparian vegetation clearing and stream cleaning of vegetation debris, which continued into the in the 1980's (Drew Baird, USBR, pers. comm., 1999), were the prominent form of channel maintenance in this reach.

3.0 HISTORY OF PRECIPITATION, FLOWS AND SEDIMENT

3.1 Precipitation History

Precipitation in the Rio Grande watershed comes in two forms: snow and rain. Although snowfall occurs in the area of the study reach, it is short lived and does not usually produce flow events in the channel whereas snowfall in the headwaters provides water for spring runoff (Figure 3). Local rainfall from thunderstorms produce short-lived sporadic flow events in the Rio Grande, and may occur throughout the year but most often in July, August and September. Each type of flow event, spring runoff and summer thunderstorm runoff, produce distinct sediment supplies: spring runoff carries a relatively low amounts of sediment, while the thunderstorm/arroyo fed summer events are rich in sediment (Figure 4).

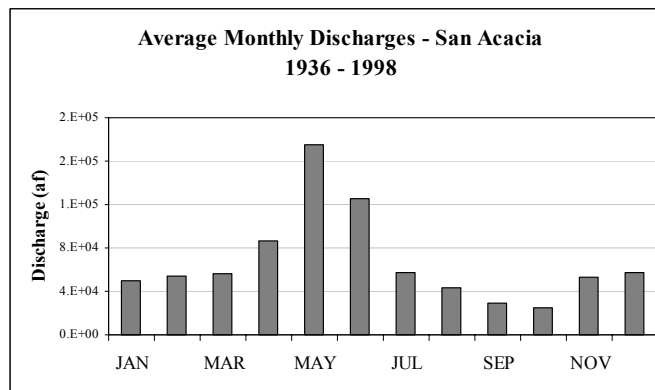


Figure 3: Average monthly discharges – USGS Rio Grande gage at the San Acacia Floodway

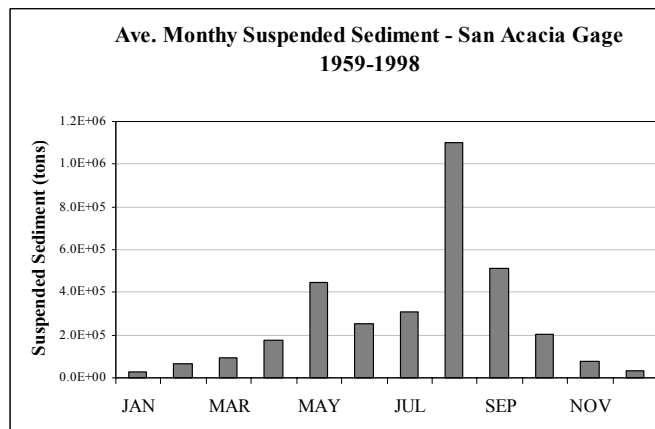


Figure 4: Average monthly suspended sediment – USGS Rio Grande gage at the San Acacia Floodway.

Although the yearly precipitation patterns are not entirely consistent between all weather station gages in the Rio Grande watershed, snow pack data indicate a relatively low pack in the mid-1970's, and returning to a larger pack in the 1980's and 1990's (Figure 5). Snow pack and mountain precipitation data was compiled for four stations in the Rio Grande headwaters

(Hydrosphere, 2000), ranging in elevation from 9,000 to 10,600 feet, and containing data from 1948 to the present (Figure 1). Wolf Creek Pass, the highest elevation gage, had the clearest trends and indicated that there was a relatively low snowfall period from about 1972 to 1977. Although data from other weather stations do not show exactly the same trends, they are not inconsistent with Wolf Creek data (Figure 5).

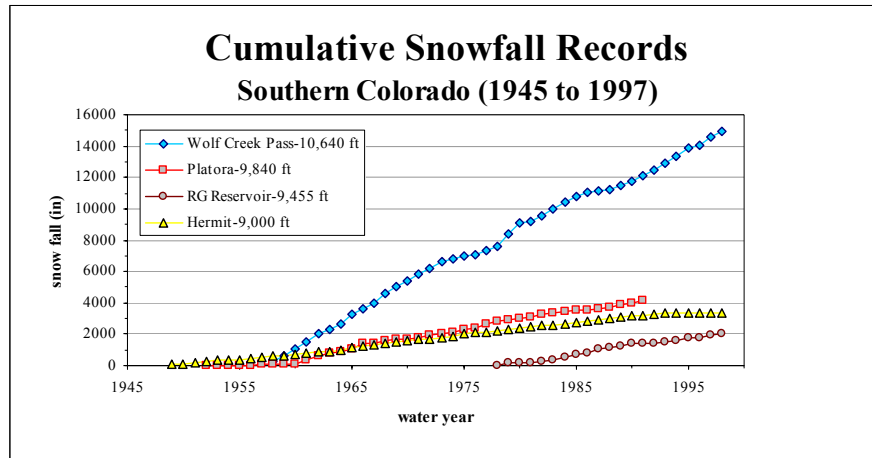


Figure 5: Cumulative snowfall records in southern Colorado.

Summer precipitation trends were assessed from the weather station data at both Socorro and Bernardo (Figure 1). Data at the Socorro station dates from 1931 to the present (Figure 6), while Bernardo station data began in 1962 (Hydrosphere, 2000). Precipitation records at both Socorro and Bernardo indicate a relatively high rainfall post-1970, but low rainfall prior to 1970. Coupled with the snow pack data, low snowfall trends in the mountains appear to be associated with relatively higher summer precipitation, and vice-versa.

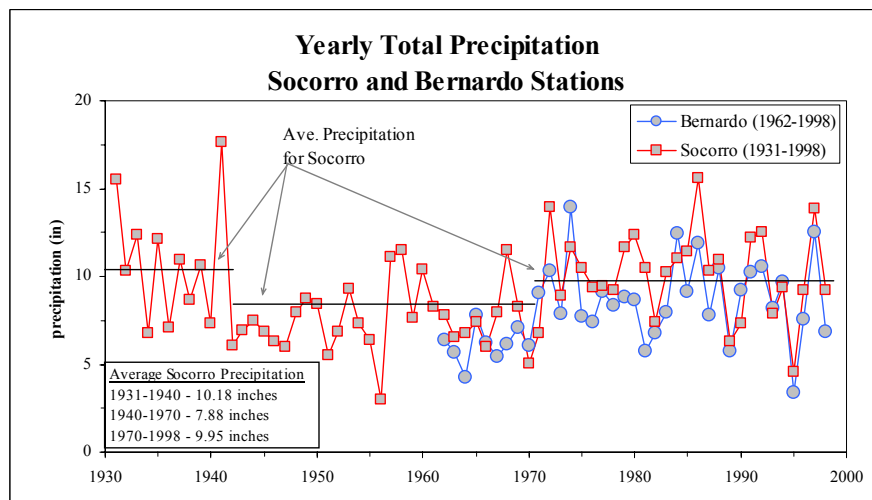


Figure 6: Yearly total precipitation at Socorro, NM and Bernardo, NM.

3.2 Gaged Stream Flow and Sediment History

Data from two USGS Rio Grande stream gages, San Acacia (# 08354900) and San Marcial (# 08358400) were used to determine the water discharge-suspended sediment history. Discharge for the San Acacia gage dates from 1936 to the present, while suspended sediment only dates back to 1949. The San Marcial gage has a more extensive record, with discharge data collected back to 1895 and suspended sediment back to 1925.

The volume of both water and sediment has varied greatly throughout the period of record for both the San Acacia and San Marcial gages. These gages receive most of their yearly flow in May and June (Figure 3), but receive most of their sediment in August (Figure 4), which is a pattern commonly referred to as the scour and fill cycle. According to data at the San Marcial gage, 1941 was as the largest water year on record while 1929 was the largest sediment year on record. Anecdotal information indicates that approximately 64 floods occurred between 1822 and 1942, and of these floods, 5 were valley filling event or flows estimated to be over 100,000 cfs (Scurlock, 1998). Annual trends of the quantity of water and suspended sediment passing the San Acacia gage indicate that the total yearly amount of water increased in the 1980's (Figure 7) while the amount of sediment has steadily decreased since 1980 (Figure 8). The concentration of suspended sediment varies significantly prior to 1978 for the San Acacia gage, ranging from 7,300 to just over 34,000 mg/l/yr (Figure 9). However, in the 1980's, the concentration of suspended sediment decreased significantly, averaging about 3,000 mg/l/yr. Since 1990, the average suspended sediment concentration at San Marcial gage is about twice the amount at the San Acacia gage indicating a source of sand-sized sediment between the two gages.

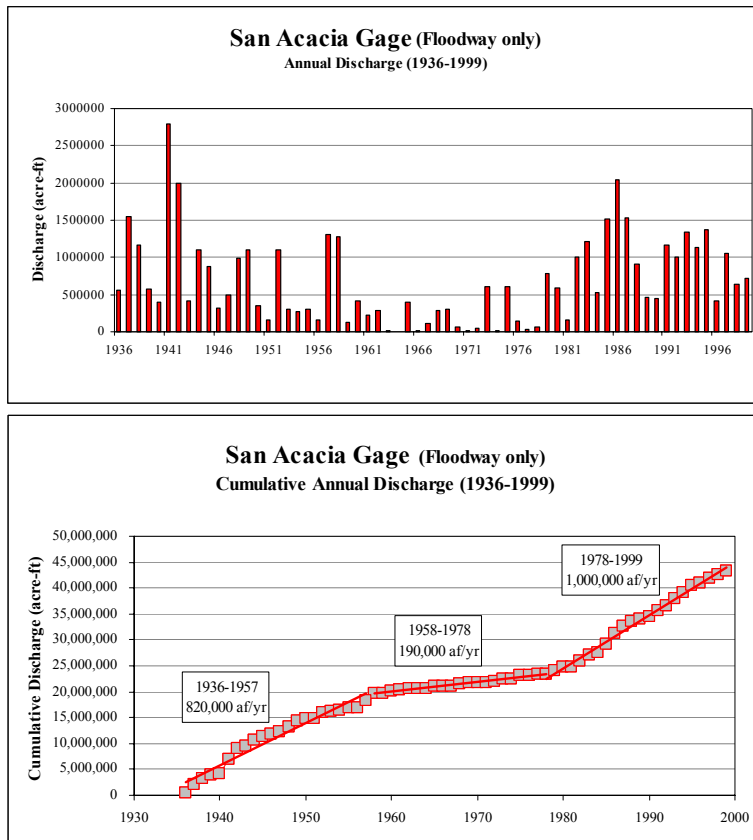


Figure 7: Annual discharge given in year discharge and cumulative – USGS Rio Grande gage at San Acacia, NM.

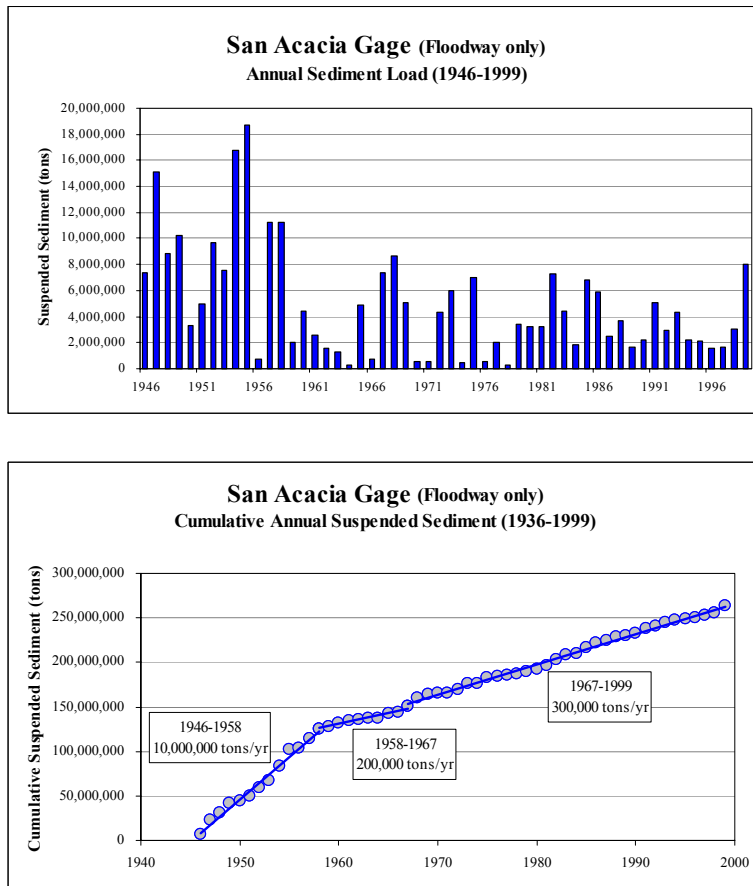


Figure 8: Annual sediment load given in year discharge and cumulative – USGS Rio Grande gage at San Acacia, NM.

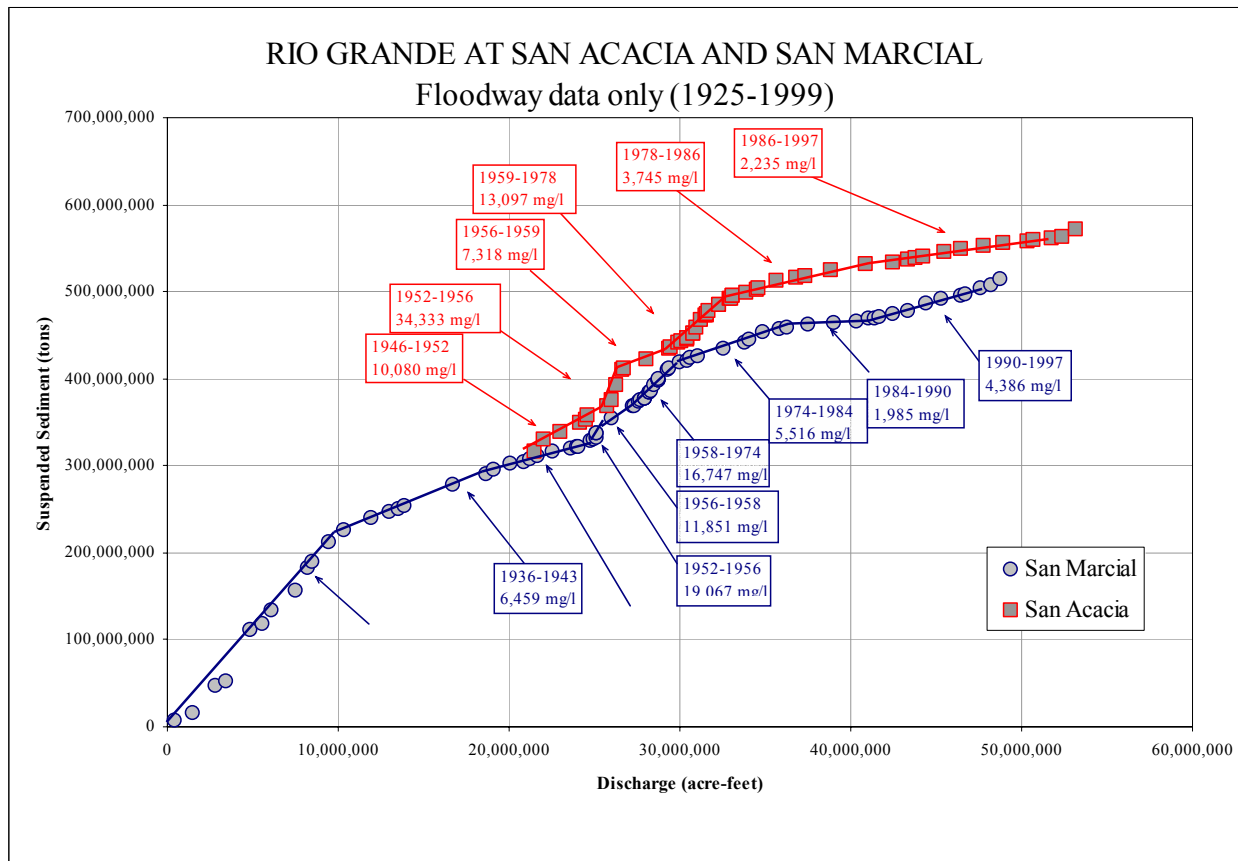
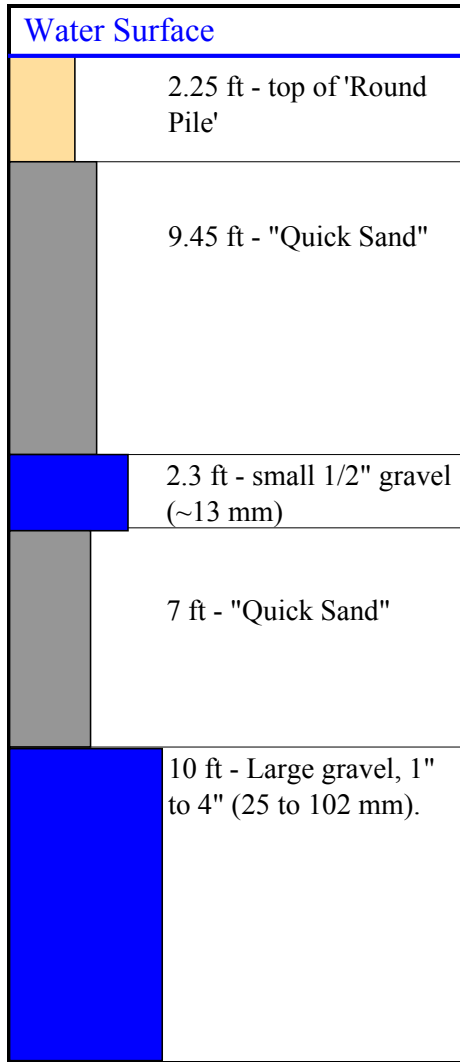


Figure 9: Cumulative suspended sediment and discharge – USGS Rio Grande gages at San Acacia, NM and San Marcial, NM.

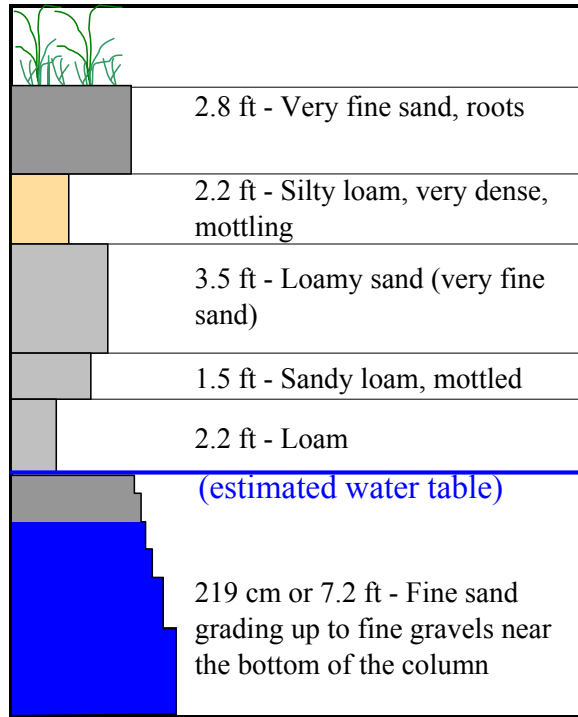
3.3 Local Supplies of Gravel and Sand

The sediment supplied by arroyos and erosion of the channel bed/banks dominates the current local supply of sediment. Wells drilled during the building of San Acacia Diversion Dam in the 1930's and a ground water study in the early 1990's (unpublished USBR data, 1930's, and 1993) found that although sand-sized sediment dominated the channel bed and bank deposits, gravel was also present (Figures 10, 11a & 11b). The gravel measured in these logs ranged from about 13 mm to 100 mm and created distinct layers, indicating that gravel sized sediment was transported in the Rio Grande, at least episodically. Logs further downstream (RM 114.6 and 109.49) found less gravel than at the dam, which may indicate that the gravel layer was spatially isolated and mostly located near its source, the Rio Salado, rather than reach wide.

RM 116.2 (@ dam), in River, 1930's



RM 114.6, next to River, 4/13/93 (CS1-1)



RM 109.49, between River and LFC, 4/3/93 (CS2-2)

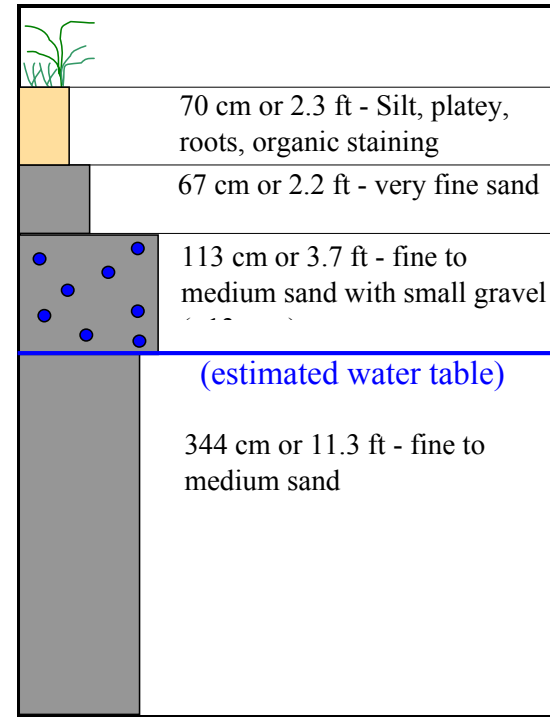


Figure 10: Historic Well Logs in the San Acacia Reach.

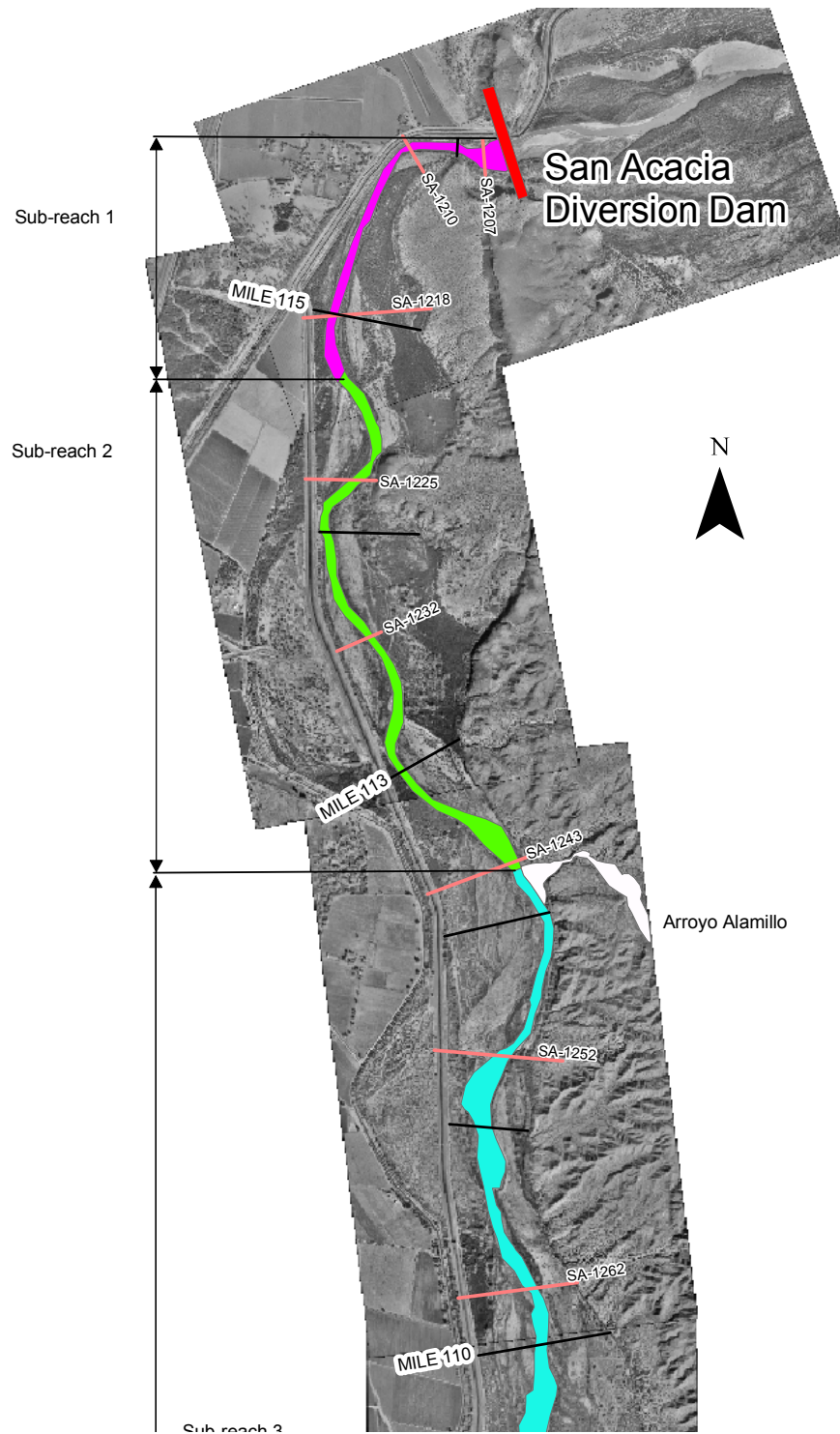


Figure 11a: Sub-Reach location map showing Sub-reaches 1, 2 and the northern portion of sub-reach 3, Rio Grande – San Acacia Reach.

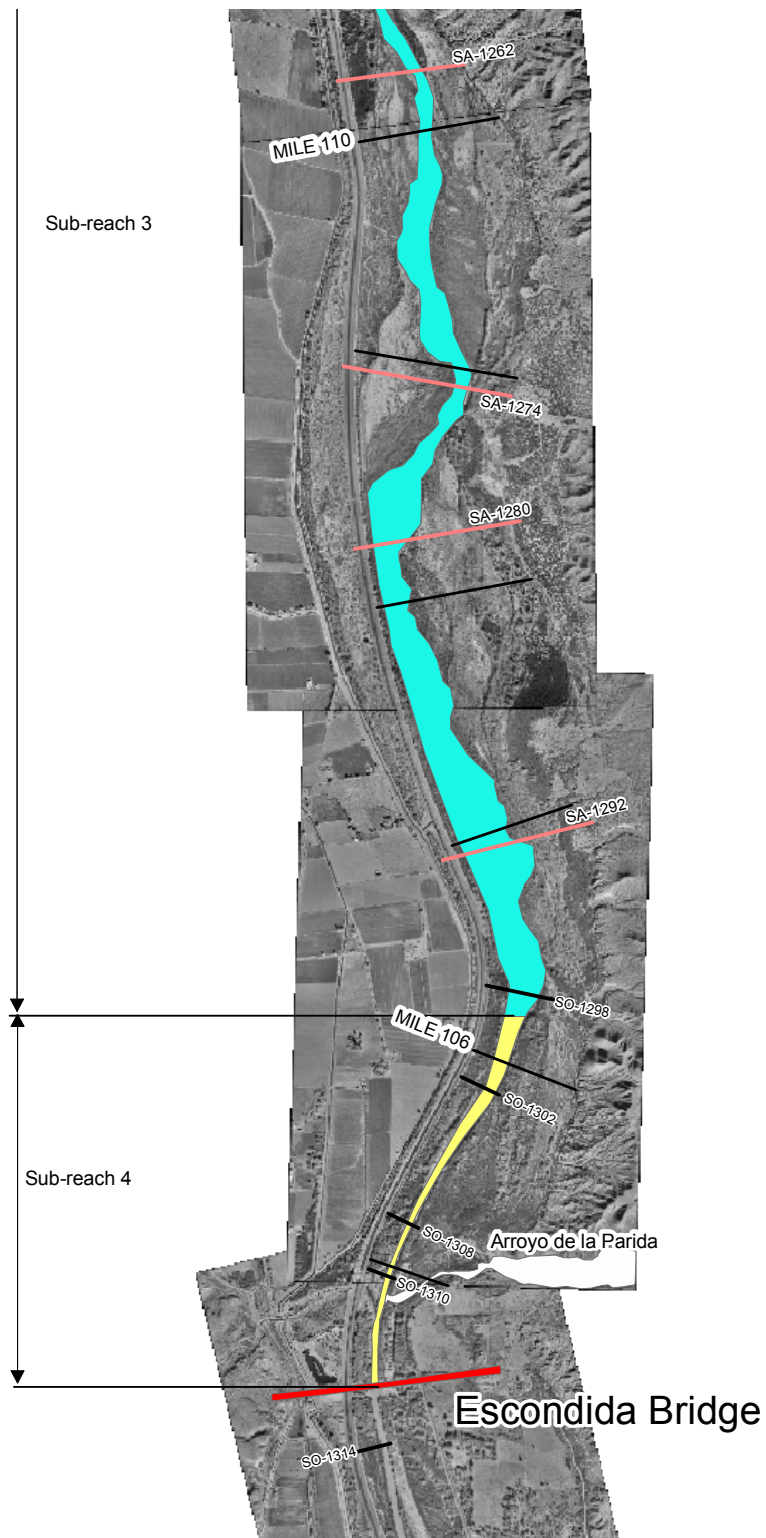


Figure 11b: Sub-Reach location map showing the southern portion of sub-reach 3 and sub-reach 4, Rio Grande – San Acacia Reach.

Large arroyos currently supplying sand and gravel sized sediment include the Rio Salado, Arroyo Alamillo and Arroyo de la Parida. Although the Rio Salado enters the Rio Grande just upstream of the study reach gravel transports to the mainstem are currently transported downstream of San Acacia diversion dam. Although historic levels of Rio Salado sediment supply are unknown, the size and present extent of the Rio Salado alluvial fan is similar to that found in earlier photos (1935 photos), indicating that the supply of sediment may have been similar throughout the 1900s. Current sediment sizes found in the Rio Salado alluvial fan consists dominantly of sand and gravel (Table 1), however cobble sized sediment from the Rio Salado were found in the Rio Grande channel immediately downstream of the confluence. Two medium-sized arroyos, Arroyo Alamillo (at RM 112) and Arroyo De La Parida (at RM 105), currently enter into the Rio Grande in this study reach (Figure 11). Both these arroyos transport sand, gravel and larger sized particles (Table 1) to the Rio Grande. San Lorenzo Arroyo, which historically meets the Rio Grande at approximately RM 113.5, was disconnected from the Rio Grande when the LFCC channel was built in the 1950s/1960s. These tributaries and relic sediment deposits in the channel bed/banks are important local sediment sources for the Rio Grande, but especially important as local sources of gravel.

Table 1: Samples of bed material from tributaries within or near the San Acacia Reach.

Tributary	Sampling method	d ₈₄ (mm)	d ₅₀ (mm)	d ₃₅ (mm)
Rio Salado	dry sieve	35	12	9
Arroyo Alamillo	dry sieve	16	7	4
Arroyo de la Parida	dry sieve	22	8	6
Arroyo de la Parida	surface count	148	93	85

4.0 RIVER CHARACTERISTICS

Analysis of five river characteristics, terraces, channel forming flows, channel morphology/pattern, dimensions of cross sections, and sediment sizes on the channel bed, indicates that the San Acacia reach has changed significantly since the early 1900's. Since channel form varies throughout this study area, the reach was divided into four sub-reaches for discussing channel form and the physical channel characteristics analysis.

Six distinct terraces were identified and mapped onto 1:400 foot 1992 orthophotos. After their locations were digitized into a geographical information system (GIS), they were compared with historic aerial photographs (1918, 1935, 1949, 1962, 1972, 1985 and 1992) to estimate a date of abandonment for each surface.

The channel forming flow was estimated using three techniques: 1-calculating the effective discharge for transporting sand sized sediment from USGS San Acacia gage data (1986-1997), 2-developing a recurrence interval for the yearly peak daily discharges (1959-1997), and 3-collecting field data to estimate the current bankfull discharge (1999). Channel patterns were described from field observations, then several classification models were applied to the study reach which included both a descriptive classification and several threshold-based models.

HEC-RAS (U.S. Army Corps of Engineers' Hydrologic Engineering Center-River Analysis System version 2.2 program 1998) and STARS (U.S. Bureau of Reclamation's Sediment Transport and River Simulation model, 1987) were used to estimate current channel characteristics from photogrammetric collected cross section data (1962, 1972 and 1992) and field collected cross data (1997 and 1999).

Bed material data were collected periodically at the USGS San Acacia gaging station, 1966 to 1999 and along the USBR San Acacia and Socorro cross section lines, 1995-1999. These data have two purposes: 1-to estimate change in particle size distribution on the channel bed over time, and 2-to estimate the sand load from upstream sources. The sand load from upstream sources was estimated using the Modified Einstein Procedure through the program *Psands* (U.S. Bureau of Reclamation, 1969).

Sediment supply from in-channel sources were estimated using two methods: 1-comparison of historic cross sections with the current cross section data and calculating the difference in volume for an average cross section scour volume, and 2-comparisons between the incoming sediment load with the estimated transport capacity of the sand sized particles.

Together, these data describe the current conditions and how they are different from the historic conditions. The data computed in this section plus the temporal trends found during the comparison between the historic and current conditions, will be used to assess and estimate future conditions.

4.1 Terraced Surfaces

Six fairly distinct abandoned alluvial surfaces were found between the San Acacia diversion dam and the Escondida bridge (Figure 12). By reviewing photos and maps dating back to 1918, approximate dates of abandonment have been estimated for most of these surfaces. Two terraces pre-date the 1918 photos, while the other four surfaces were either within the active channel or floodplain in 1918. Using the U.S. Army Corps of Engineers' Hydrologic Engineering Center-River Analysis System (HEC-RAS) version 2.2 program (USACE, 1998) with field surveyed cross section profiles, water discharge magnitudes were estimated for flooding each of these terraced surfaces, except Terrace 1 due to insufficient survey data. Due to a 'fixed-bed' assumption in the model (the elevation of the channel bed does not change with increasing discharge), estimates of the size of flooding flows are likely low. For example, the HEC-RAS model estimated that Terrace 6, the 3 foot surface, floods at 5,000 cfs, whereas, field observations indicate that a recent flow with an instantaneous peak greater than 5,000 did not flood this surface. Surface elevations for each set of terraces were estimated using the 1992 cross section data set. Since terraced surfaces do not maintain a constant elevation downstream from its first occurrence, the elevation from the most upstream surface is reported.

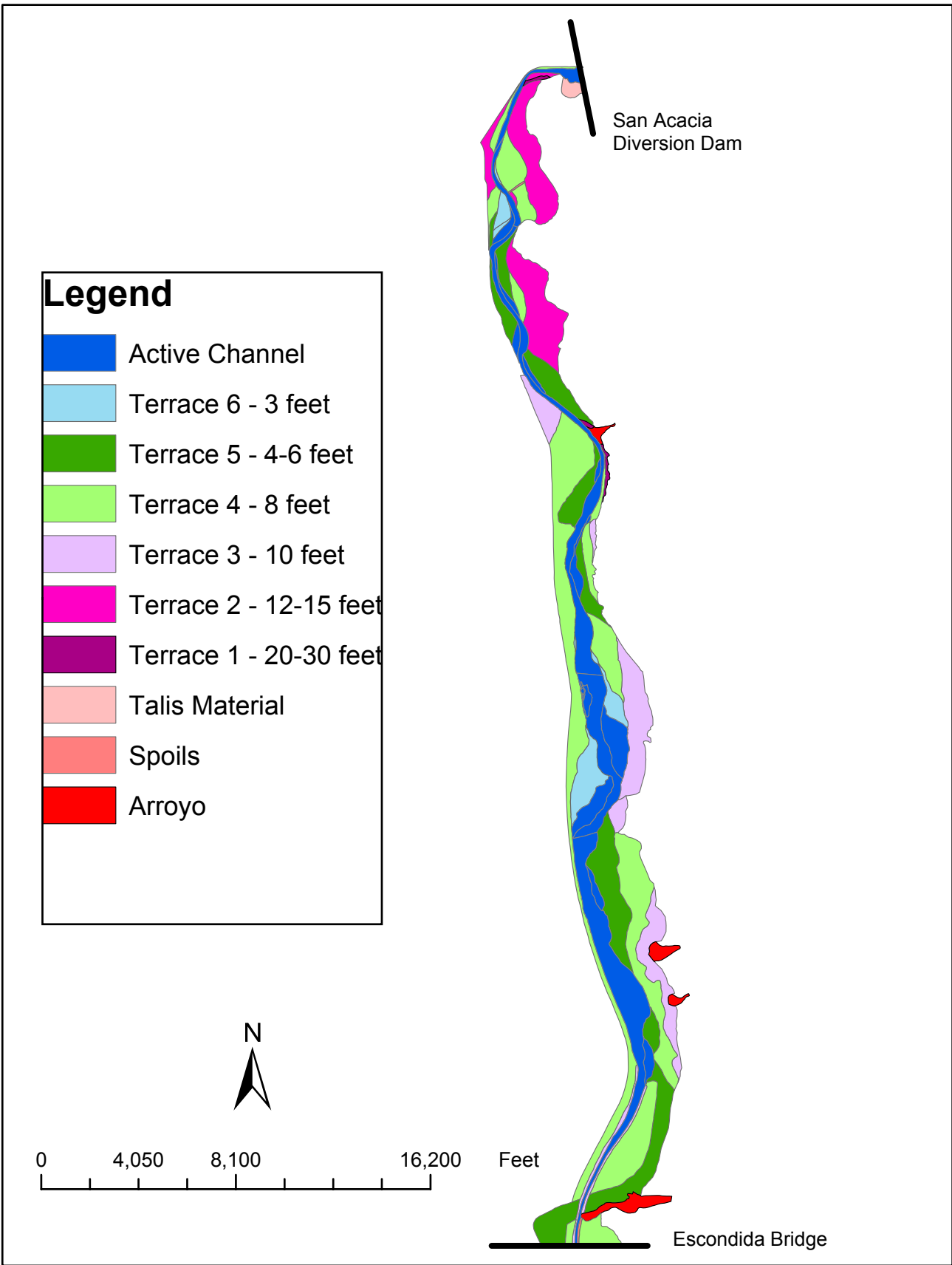


Figure 12: Terraced surfaces along the Rio Grande – San Acacia Reach.

4.1.1 Terrace 1 and 2

The highest terrace (Terrace 1), and presumably the oldest, is approximately 30 feet higher than the active channel. This terrace comprises less than 1% of the terraces mapped, and was found in only two locations: near the diversion dam, and at the mouth of Arroyo Alamillo (Figure 12). Terrace 1 near the diversion dam is a strath terrace, where fluvial sediments of gravel, sand and silt were deposited on top of an eroded bedrock surface. The Terrace 1 surface located at the confluence of Arroyo Alamillo, is a pinkish colored alluvial terrace composed of poorly sorted gravel, sand and silt sediments.

The second highest terrace, Terrace 2, ranges from 12-15 feet above the active channel height and is most commonly located along the base of the east mesa just downstream of the diversion dam. Terrace 2 is composed of alluvial deposits and comprises approximately 12% of the area mapped as terraces. Both Terrace 1 and Terrace 2 were formed prior to 1918, therefore determining their specific ages is not possible from the currently available historic data. Results from the HEC-RAS model for Terrace 2 indicate that an average flow of 36,000 cfs would over-top this terrace (Table 2).

Table 2: Summary information for the San Acacia Reach terraces.

Terrace #	Terrace Height above River Level	Terrace Elevation	Total Area of Terrace	Est. Flow Size to Flood Terrace
1	20-30 ft	N/D	11 acres	N/A
2	12-15 ft	4673 ft	290 acres	36,000 cfs
3	10 ft	4653 ft	320 acres	32,000 cfs
4	8 ft	4675 ft	1200 acres	24,000 cfs
5	4-6 ft	4655 ft	510 acres	14,000 cfs
6	3 ft	4651 ft	160 acres	5,000 cfs

4.1.2 Terrace 3 and 4

Terrace 3, a 10 foot high terrace occurs most often along the east side of the current floodway. This surface appears to have been the active floodplain in 1918; it was abandoned by 1935 (> 65 years old). Vegetation present consists of mature cottonwoods, tamarisk, grasses and small brush. This terrace contains distinct layers of sand, silt, and clay. The sand and several of the silt layers have well preserved cross-bedding features and appear to be moderately well sorted. The sand layers are located relatively deep in the profile, while the finer grained material, consistent with floodplain deposits, are higher in the stratigraphic column (Figure 13). This terrace often forms vertical banks and is estimated to flood at 32,000 cfs.

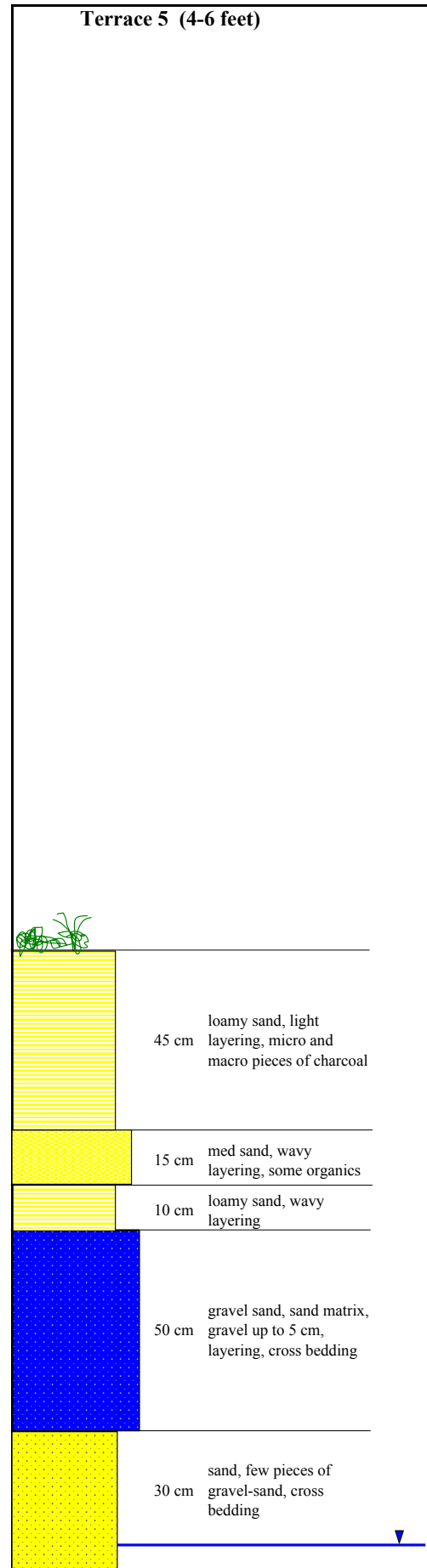
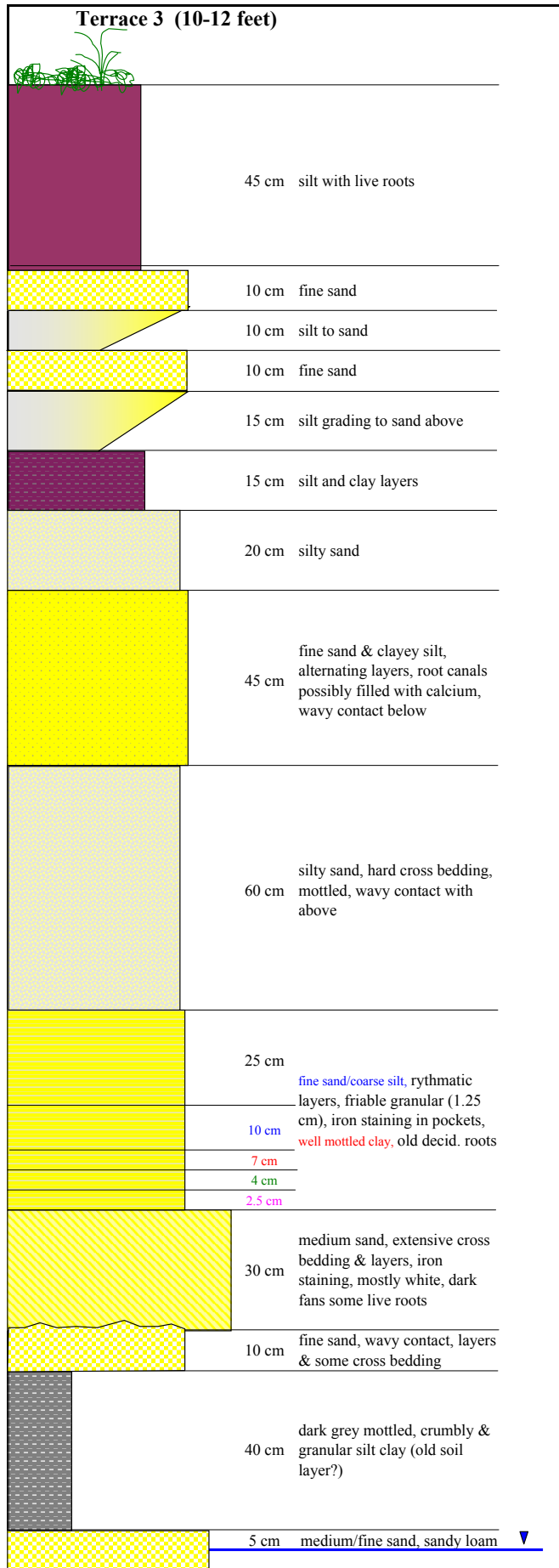


Figure 13: Terraced surfaces along the Rio Grande – San Acacia Reach.

The 8 foot terrace (Terrace 4) is the most abundantly found terrace in the San Acacia reach, comprising almost 50% of the mapped area. In 1918 this surface was completely within the active channel, however by 1935 much of the surface was already exposed, and by 1949, this surface was completely abandoned (50-65 years old). Vegetation on this surface is comprised of mature cottonwood stands, dense tamarisk stands, shrubs, grasses and cacti. Thick sand and/or silt layers dominate the sediments in this terrace. Several layers have gravel sized material in them, but most are composed of silty-sands or sands. This terrace forms banks that have vertical sides for 2-3 feet, while the remaining 5-6 feet of the terrace is buried beneath eroded bank material forming a sandy fan. The HEC-RAS model estimates surface flooding to occur at approximately 24,000 cfs.

4.1.3 Terrace 5 and 6

Like the 8 foot terrace, the 4 to 6 foot terrace (Terrace 5) is a common surface in the San Acacia reach, but is composed of more sand and gravel materials than Terrace 4 (Figure 13). This surface was active channel in the 1972 photos, but by the 1985 photos, it was completely abandoned (15-28 years old). The vegetation on this terrace consists mostly of grasses and young trees (10-20 feet tall). The 4-6 foot terrace is composed of loamy sand, sand, and sand/gravel mixtures (Figure 13). The sediment layers have a loose, non-cohesive structure. This terrace forms angled banks that are composed of eroded terrace sediments: the terrace is estimated to flood at 14,000 cfs.

The most recently formed terrace (Terrace 6) is approximately 3 feet higher than the current active channel. Although this surface is close to the present channel, the flood in August 1999, which was a bank-filling event, did not inundate this surface, thus indicating that it is not the active floodplain. In the 1985 photos, this surface is completely within the active channel, but by the 1992 photos, it is completely abandoned (8-15 years old). Vegetation present on this terrace consists mostly of young willows, cottonwoods, grasses and some tamarisk seedlings. Sand and gravel sized sediments compose this terrace, which have no internal cohesion. Although HEC-RAS predicted this terrace to flood at approximately 5,000 cfs, field evidence from the August flood indicated that a 7,000 cfs instantaneous peak flow did not wet this surface. These data indicate that the HEC-RAS model under estimates the flows required to flood the terraced surfaces.

4.1.4 Terrace Summary

Terraces 1, 2, 3 and 4 were all abandoned prior to significant channel modifications such as the construction of the LFCC, building of the levee system and channelization activities. These terraces comprise 1821 acres or 73 % of the mapped area. Both Terraces 5 and 6 were abandoned in recent history: Terrace 5 was abandoned between 1972 and 1985, while Terrace 6 was abandoned between 1985 and 1992. Both terraces post date construction of the LFCC and major channelization efforts. They comprise approximately 670 acres.

4.2 Channel Forming Flow

The channel forming discharge or dominant discharge, is the discharge “which determines particular channel parameters” (Knighton, 1998) such as sinuosity, channel depth, width and sediment size. Wolman and Leopold (1957) define the channel forming discharge as simply the flow that fills up the channel (bankfull), while Wolman and Miller (1960) describe it as that flow which performs the most work in terms of sediment transport (effective flow). Others define it as the most dominant flow with a recurrence interval of 1-3 years (Leopold *et al.*, 1964, Hey, 1975, Biedenharn *et al.*, 1987, and Knighton, 1998). Since two distinct sediment sizes are present in this reach, the use of all three methods is necessary. The effective flow method will be used to estimate the flow in which the most sand sized sediment is transported, while the recurrence interval method along with bankfull discharge estimates from current field data are used for determining the channel forming flow for the gravel layer.

The flow at which the most sand sized sediment is transported, effective flow, ranged from 2,800 to 3,200 cfs for the spring flow data. Effective discharge was calculated comparing the frequency of each discharge with the amount of sediment it transported (Strand and Pemberton, 1982; and Wolman and Miller, 1960). Field observations (Bill Fullerton, Tetra Tech Inc., pers. comm., 2000) indicated that sand sized material was transported as bed load for flows greater than 300 cfs, becoming more suspended with larger flows, therefore, flows <300 cfs were not analyzed for effective flow. Comparing the shear to fall velocities, u^*/ω (Julien, 1995), indicates that a discharge of 3,000 cfs transports sand sized particles as suspended sediment for all sub-reaches. Since the sediment to discharge relationship is not consistent over the period of record (Figure 9), the current conditions for effective discharge were determined using data from 1986-1997 only. A discharge of approximately 3,200 cfs was estimated to move the most sediment during spring runoff, while a flow of 2,800 cfs during summer runoff transported the most sediment (Table 3). Since field evidence indicates that 3,200 cfs is significantly below a bankfull discharge, this estimate was only used for the analysis of the sand sized sediment supply.

Table 3: Effective discharge calculations, USGS Rio Grande gage at San Acacia.

Discharge (cfs)	# Flows in Data Set	Cumulative Suspended Sediment (tons/day)	Ave. Concentration per Flow (mg/l)
Spring Flows			
5200	26	296,000	900
5000	29	197,300	560
4400	53	462,700	810
3600	61	413,100	770
3200	60	488,400	1,040
3000	58	464,500	1,090
2800	46	299,200	950
2600	66	329,300	780
Summer Flows			
5000	9	506,600	4,600
4000	18	807,100	4,580
2800	15	1,326,000	12,900
2600	15	912,400	9,560
2000	17	913,800	10,990

Since data are not available to estimate the effective flow of the gravel sized particles, field collected bankfull data and a flow event frequency analysis (recurrence interval) were used to estimate the channel forming event, which was estimated at approximately 5,000 cfs. Since a complete record of instantaneous peaks are unavailable through the 1990's, mean daily discharge data were used for the recurrence interval assessment. Discharge data from both 1959-1979, a relatively dry period, and 1979-1997, a relatively wet period, indicate that a flow of 5,000 cfs has a recurrence interval of 1.5 to 2.5 years (Figure 14). Both data sets show that the frequency-discharge relationship changes at approximately 5,000 cfs, such that higher than 5,000 cfs, small changes in discharge correlate to large changes in the recurrence interval. This shift in frequency-discharge trend, as well as the pivot point at 5,000 cfs persists regardless of the wet-dry period, thus suggesting that the 'average flood' has remained constant in size if not frequency even with other influences such as climate. In August, 1999, a flow event with a mean daily discharge of about 5,000 cfs and an instantaneous peak of about 7,000 cfs passed the USGS San Acacia gage; from field data collected after the event, this flow was approximately a bank filling event (a bankfull event). Bankfull indicators included: observed over bank flooding locations consistent with low floodplains, height of flow marks on non-flooded banks, inundation of previously formed bars and the height of newly formed bars. Using both the recurrence interval data and the field data from the August 1999 event, a flow of 5,000 cfs,

which appears to be controlling channel morphology, is estimated to be the channel forming event.

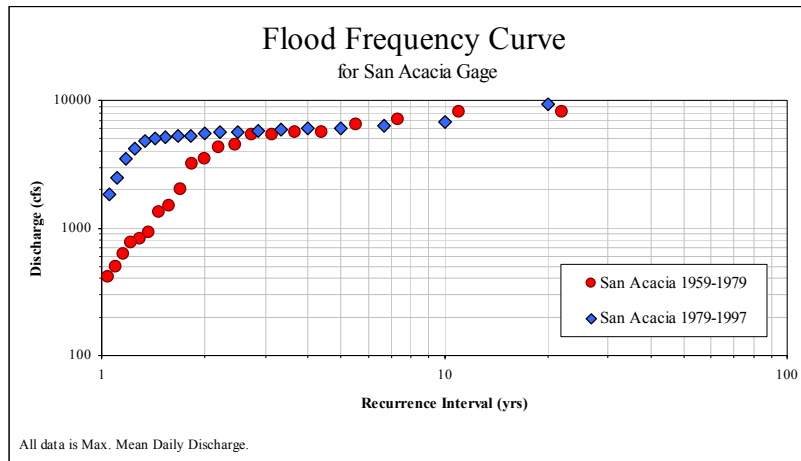


Figure 14: Flood frequency curve, Rio Grande – San Acacia Reach.

4.3 Sub-Reach Designation and Channel Classification

The San Acacia reach was divided into four sub-reaches (Table 4). For sub-division of the reach, channel width was estimated from historic and current photographs. Photographs from 1992 were reviewed along with field visits to determine changes in general channel patterns. Channel elevations from field measured cross sections in 1997 were used to determine breaks in longitudinal slope. A history of channelization activities was also used in determining the sub-division the reach.

Table 4: Sub-reach description and lengths.

	Brief Description	Sub-Reach Lengths		Range Lines
sub-reach 1:	straight and narrow	6,800 ft	1.3 mi	1207-1221
sub-reach 2:	slightly sinuous and narrow	11,600 ft	2.2 mi	1221-1243
sub-reach 3:	mostly straight and wide	30,200 ft	5.7 mi	1243-1298
sub-reach 4:	straight and narrow	7,400 ft	1.4 mi	1298-1316
Reach Total:		56,000 ft	10.6 mi	

4.3.1 Reach and Sub-Reach Descriptions

At present, the general character of the whole reach consists of two dominant morphologies: 1) a mostly straight, narrow, single channel (51% of the total reach length); and 2) a wide, mostly straight, active channel that alternates between a single threaded channel and a braided morphology. In its present location, east (left) side of the river valley, the channel is confined by outcrops of bedrock (sedimentary and igneous), high terraces, levees, and railroad tracks. Channel slope ranges from 0.00029 to 0.0028, ft/ft with an average of 0.0008 ft/ft.

Although the channel is generally straight (Figures 15 and 16), several sections have developed point bars and a slight meandering channel pattern. Since the 1930's, channel width in the entire reach has steadily decreased (Figures 15 and 17). The bed material has a bimodal sediment size distribution, consisting of both sand and gravel sediment. The river channel in the first four river miles (from the diversion dam to Arroyo Alamillo, Figure 11) contains a fairly consistent gravel layer, covered by 2-3 feet of sand. Downstream of Arroyo Alamillo the gravel layer is intermittent, and is usually covered by a thick layer of sand (3+ feet). Other than the building of the San Acacia Diversion Dam (see Human Influences section) local channel modifications include channel straightening (1956-1959), riparian brushing (until the mid-1980's) and stream cleaning and grading, which ended in about 1985, (Drew Baird, USBR, pers comm., 1999).

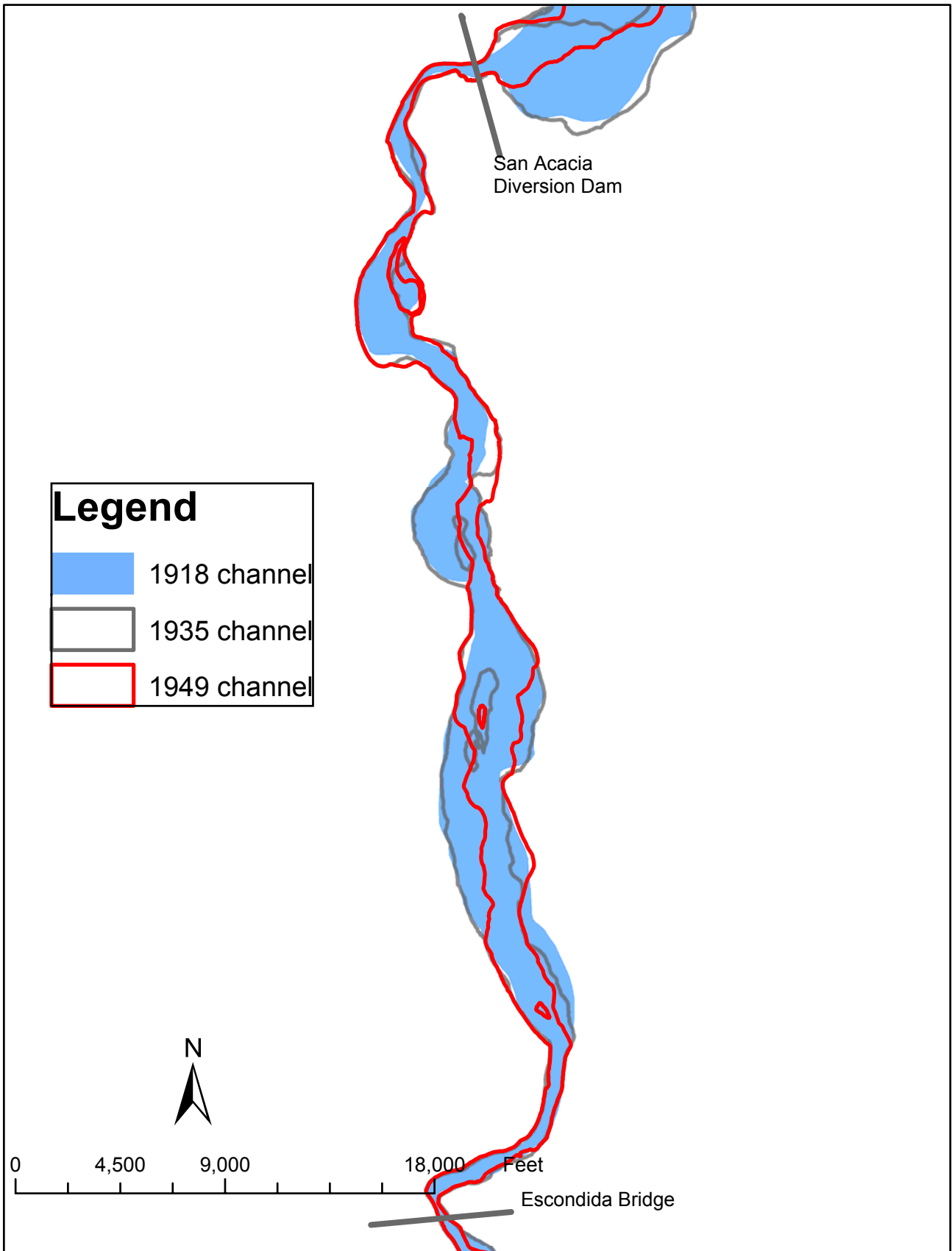


Figure 15A: Historic trends in channel location, Rio Grande – San Acacia Reach: 1918, 1935, 1949 channel locations.

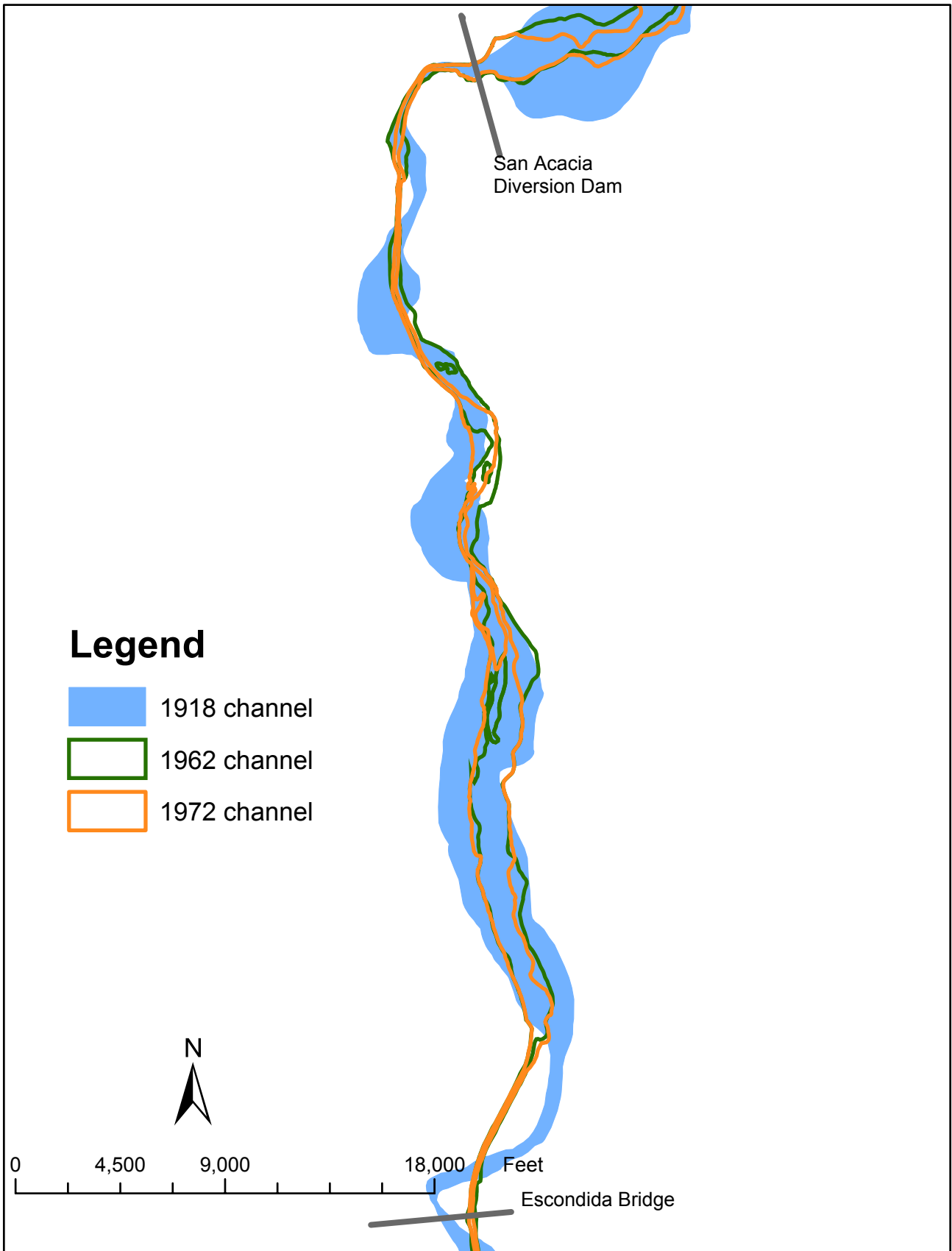


Figure 15b: Historic trends in channel location, Rio Grande – San Acacia Reach: 1918, 1962, 1972 channel locations.

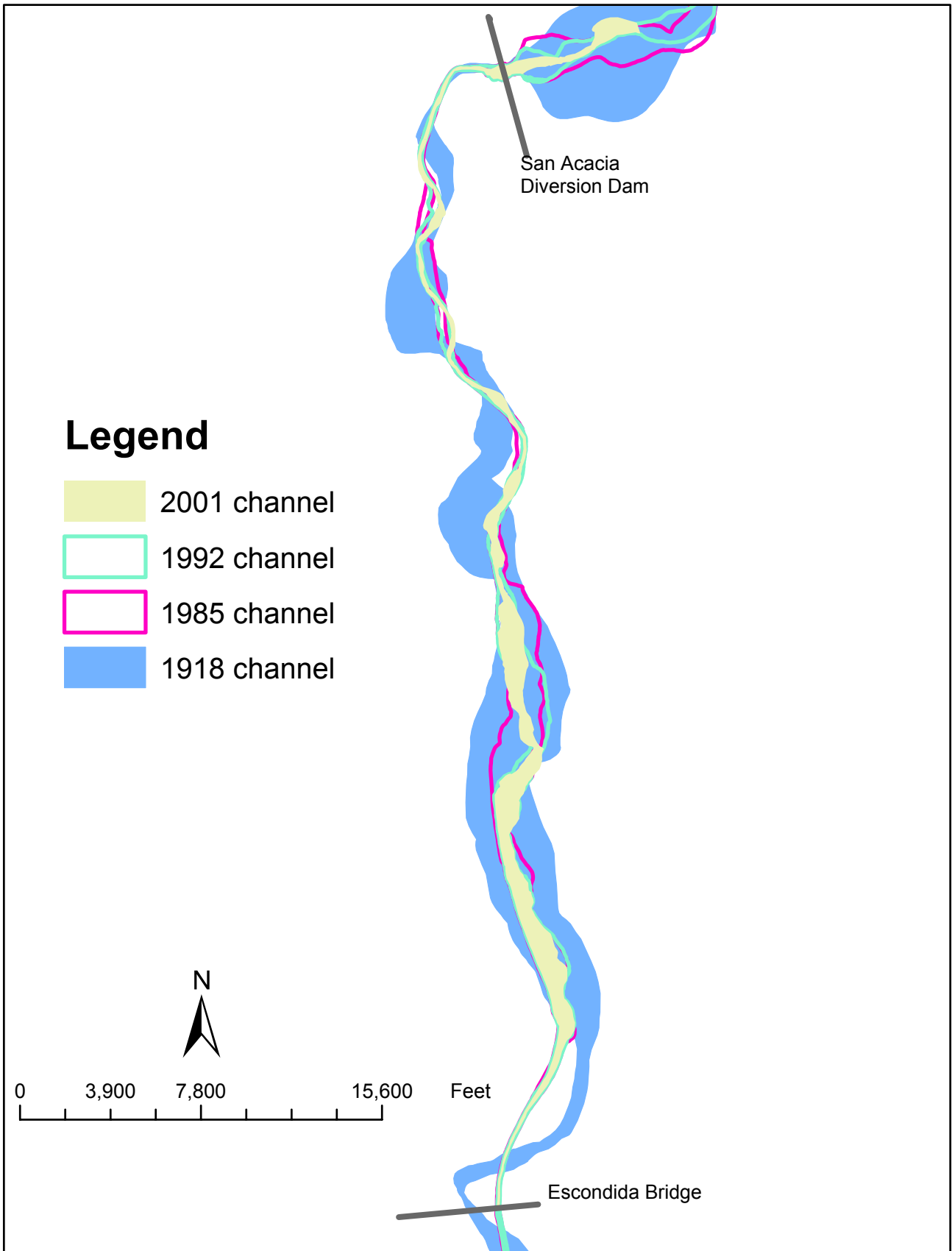


Figure 15c: Historic trends in channel location, Rio Grande – San Acacia Reach: 1918, 1985, 1992 and 2002 channel locations.

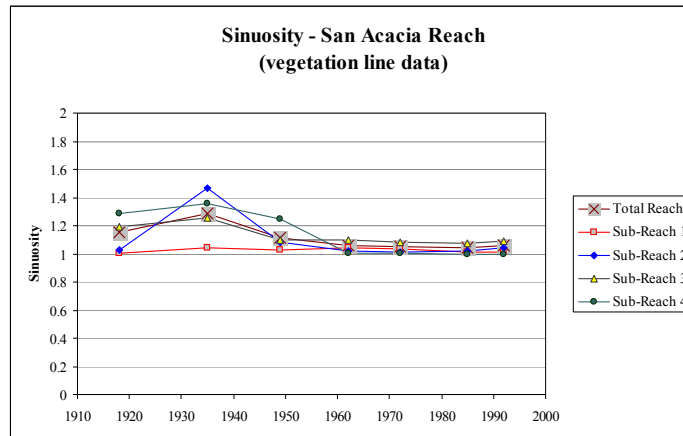


Figure 16: Historic trends in channel Sinuosity, Rio Grande – San Acacia Reach.

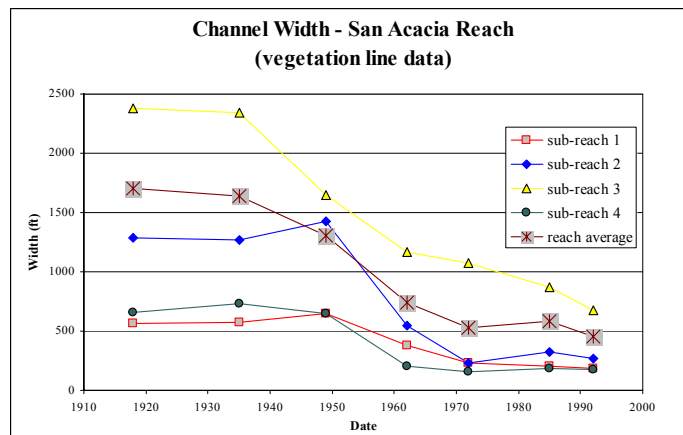


Figure 17: Historic channel width, Rio Grande – San Acacia Reach.

Sub-reach 1 is a straight, single threaded channel morphology that is relatively narrow and deep (Figures 14-15). This morphology does not change with discharge. The channel is tightly confined by bedrock and terraces on the left, and by terraces, railroad tracks and levees located on the right side of the river. The channel width has decreased from about 550 feet in 1918 to about 200 feet in 1999 (Table 5). The current channel slope is 0.00084 ft/ft. A layer of gravel lines the channel bed in this sub-reach, which likely moves only in channel forming flows. The sand layer that blankets the gravel moves through the sub-reach during almost all flows. During low flows, the sand is transported downstream in dune fields. Channelization efforts in this stretch of the river began in the 1930's with the building of the diversion dam and were at their height in the 1950's with the building of the LFCC. Additional channelization continued into the early 1980's.

Table 5: Summary of active channel widths in feet, by year, as measured from the distance between riparian vegetation on historic aerial photos, San Acacia Reach.

	1918	1935	1949	1962	1972	1985	1992
sub-reach 1	570	570	650	380	230	200	190
sub-reach 2	1290	1270	1420	550	230	320	270
sub-reach 3	2380	2340	1650	1160	1070	870	680
sub-reach 4	660	730	650	200	160	190	170
REACH AVERAGE:	1670	1660	1320	790	650	580	460

Sub-reach 2 is a slightly sinuous, single-thread channel (Figures 14-15) during both high and low flows. Due to the recent development of point bars and the slightly meandering pattern, the channel width varies slightly within this sub-reach. The development of larger meander bends is retarded by the confinement of the river by tall terraces, bedrock, and the west-side levee. The current channel slope is 0.00070 ft/ft. Similar to sub-reach 1, this channel contains a bi-modal sediment distribution of gravel and sand. The gravel size fraction forms a continuous layer defining the channel bed, while the sand size fraction forms a blanket of finer sediment covering the gravel layer. Sand sized particles are transported throughout all flow regimes above 300 cfs. Channelization activities between 1949 and 1962 (LFCC construction) reduced the channel width (Table 5) and moved the channel to its present location.

Sub-reach 3 is the only sub-reach to have maintained a channel form similar to historic conditions; however, channel patterns appear to be evolving from a mostly braided form to a meandering form. Since 1992, the upstream 2 miles has converted to a channel pattern similar to the meandering form of sub-reach 2, while channel form in the remaining 3.5 miles is still the low-flow braided form. As flows approach channel full, sub-reach 3 becomes a single-threaded channel as the sediment bars are inundated. Although this sub-reach has narrowed by almost 1,700 feet, it still has the largest average width in the study area, 680 feet in 1992 (Table 5). Although the current channel slope averages only 0.00073 ft/ft, this sub-reach has the steepest sloped sections of the river in the reach. Competent gravel layers were measured in this sub-reach, however, the gravel layer is not continuous in either cross sections nor in longitudinal profiles. As observed in the other sub-reaches, the sand sized particles are easily transported above 300 cfs. Although extensive lateral migration of the river is still limited by the location of the east valley wall, alluvial terraces and the levee, the distance between these migration barriers is greatest in this sub-reach. The only channel modifications apparent in this sub-reach occurred in the 1950's, in which the west side bends were truncated and emplacement of jetty jack fields decreased channel width.

The effects of re-alignment and channelization activities in the late 1950's (Figure 15) dominate channel form in sub-reach 4. With the building of the LFCC, a set of meander bends was cut off in order to create a straight channel pattern: sub-reach 4 continues to flow exclusively in the constructed channel. Banks heightened by the spoils of the dug channel confine the channel. The current channel is straight and deep and has maintained about the same channel width since 1962 (Table 4). This sub-reach has the steepest average slope at 0.0014 ft/ft. No

bars, point or medial, have developed since channelization, and the bed is mostly composed of sand dunes at low flows and plane-bed, upper regime at higher flows.

4.3.2 Rosgen's Description Based Classification Model

The Rosgen (1996) stream classification system does not readily fit the channel forms found in the San Acacia reach. Prior to the 1950's, most of the reach would have been classified as a D5 stream type: braided, channel slope equals valley slope (<0.04), low sinuosity, not incised, sand dominated bed, with a significant floodplain. However, at present, the floodplain has been abandoned, initially by the building of levees, but now by channel bed incision. Although sand is still present, much of the reach is gravel bedded, and almost half the reach is no longer braided. Only the widest sections in sub-reach 3 may still be considered a D5 stream type with some exceptions of D5 channel features, such as access to a floodplain.

Sub-reach 1 and sub-reach 2 fit into Rosgen's classification between a F4 and a F5 stream type, however several of the physical features in the channel are not consistent with either classification. The F-series stream types are deeply incised streams, downcutting through gentle gradient valleys, structurally controlled, that have low slopes and high width to depth ratios. An F4 is a gravel bedded channel, slope less than 0.02, width/depth ratio >12 , an entrenchment ratio <1.4 and a sinuosity >1.4 . An F5 has similar characteristics, but is sand dominated. Although both sub-reaches 1 and 2 have gravel beds, much of the year the gravel is covered by sand. Neither sub-reach has a discernable floodplain (low entrenchment ratio). Both sub-reaches have high width/depth ratios (28 and 57 respectively), and slopes far less than 0.02. The main feature that does not fit from the F-series is the sinuosity, which should be >1.4 for both the F4 and F5 classifications. Both sub-reaches have sinuosities of less than 1.1.

The upper 2 miles of sub-reach 3 demonstrates physical characteristics close to an F5, while the lower 4 miles exhibits feature similar to a D5. As with sub-reaches 1 and 2, the major exception of the F5 classification in the first 2 miles of sub-reach 3 is the sinuosity. This section of channel is straight, a sinuosity <1.1 . The last 4 miles of sub-reach 3 are also straight, but dominantly by a low-flow braided pattern. The D5 stream type is described as a sand dominated channel, braided, not incised, slopes <0.04 ft/ft, high width to depth ratio and straight. The major characteristic that does not fit a D5 classification is the amount of incision. These channels, like elsewhere in the reach, have incised through fluvial sediments, thus creating terraces that confine the channel. Access and/or development of a floodplain is limited.

Since sub-reach 4 is not a 'natural' channel, Rosgen's classification system is not designed to describe this channel well. The best classification is an F5 channel type. This channel is low gradient, has no floodplain and has a width to depth ratio of almost 30. Like sub-reaches 1 and 2, the current channel pattern is too straight for this classification; it has a sinuosity of less than 1.1, versus the >1.4 for the classification. Unlike the classification description of an all sand channel, the channel bed and banks are composed of both sand and silt, while discrete deposits of gravel are found at the arroyo confluence.

4.3.3 Empirical Classification Models

Many channel classification schemes and models have been published for naturally evolving river channels which assess channel pattern: seven empirically based models are used for describing channel pattern in the San Acacia reach. The three main descriptions utilized by most classification systems for alluvial streams are braided, meandering/sinuuous, and straight. Other classification model descriptions are transitional channels, and single versus multiple channels. Most of these classification models focus on discharge (Q) and slope (S) relationships or thresholds, however, three models use relationships that relate median grain size (d_{50}), width (w), depth (d), Froude Number (F) or stream power to channel patterns.

Of the 7 empirical classification models, Parker (1976) best describes channel form for the sub-reach scale (Table 6). According to Parker’s model, sub-reach 1 and 4 are close to the transition between straight and meandering, while sub-reach 2 is well within the meandering zone, and sub-reach 3 is braided. This model’s results agree well with field observations. Of the remaining classification models, the Van den Berg (1995) classification model produced the poorest correlation with field observed channel patterns.

Table 6: Classification assigned to each sub-reach by each model.

Classification Assigned by Models					
Model	Sub-reach 1	Sub-reach 2	Sub-reach 3	Sub-reach 4	Entire Reach
<i>Leopold and Wolman (1957)</i>	not-braided	braided	braided	not-braided	braided
<i>Lane (1957)</i>	transitional	transitional	braided	transitional	transitional
<i>Henderson (1963)</i>	meandering	meandering	meandering	braided	meandering
<i>Schumm and Khan (1972)</i>	straight	straight	meandering	straight	meandering
<i>Parker (1976)</i>	straight/ meandering	meandering	braided	straight	meandering
<i>Ackers and Charlton (1979)</i>	straight with alt. bars	meandering	meandering	straight with alt. bars	meandering
<i>Van den Berg (1995)</i>	single-thread	single-thread	single-thread	single-thread	single-thread
<i>Field Observed Patterns</i>	straight, single thread	slightly meandering, single thread	straight, braided at low flows	straight, single thread	n/a

4.4 Current and Historic Cross Section Dimensions

Cross sections were examined to determine rates of change in channel parameters, such as width, depth, channel area and sinuosity using both the location of riparian vegetation on historic aerial photo, photo-measured cross section data and field-measured cross section surveys with hydraulic applications (HEC-RAS and STARS). The riparian boundary data (1918-1992)

were used to estimate both active channel widths and sinuosity of the channel. Channel width is calculated as a weighted average, while sinuosity is the ratio of thalweg length versus valley length for a given section

The applications, HEC-RAS and STARS, use cross section data collected from both historic aerial photographs (1962, 1972, and 1992) and from field surveys (1997 and 1999) to estimate the dimensions of channel parameters such as depth and channel area. Cross section data (1962-1999), along with the estimated channel forming flow of 5,000 cfs were modeled using the U.S. Army Corps of Engineers' Hydrologic Engineering Center-River Analysis System (HEC-RAS) version 2.2 program (USACE, 1998). HEC-RAS is a one-dimensional, 'back-water' model, which assumes that the channel form and channel elevation does not change while routing flows ('fixed length' and 'fixed bed'). Surveyed cross sections, length between cross sections, channel roughness (Manning's n) and the designation of channel boundaries data are required for this model. Results from HEC-RAS include cross section average values for: 1) total top width (this width is a combination of both the width of the channel and the estimated width of over bank flooding), 2) top width of the channel (over bank flooding is not included in these values), 3) maximum depth, 4) average depth (or hydraulic radius), 5) channel area, 6) wetted perimeter, 7) velocity and 8) mean bed elevation. The U.S. Bureau of Reclamation's Sediment Transport and River Simulation (STARS) model (Orvis and Randle, 1987) is a quasi-two dimensional model that also assumes a 'fixed bed', but estimates channel dimensions by routing flow through 10 flow tubes. Data requirements for the STARS model are similar to those required for HEC-RAS, however, seven flows (200, 500, 1000, 2000, 3000, 5000, 7000 cfs) were modeled using STARS for the most recent cross section data set. Therefore, while HEC-RAS model results estimate changes in channel form over time (37 years), STARS estimates changes in the 1999 channel with an increasing flow (from 200 to 7,000 cfs). Model results from STARS include: 1) width, 2) depth, 3) area and 4) velocity. For both models, results are summarized for the entire reach and then by each sub-reach. These summary values are the averages of cross section values weighted by distance between each cross section.

4.4.1 Average Reach Conditions

As a whole, the Rio Grande in the San Acacia Reach has changed significantly in both channel form and channel dimensions since 1918. Among those channel parameters that have changed, sinuosity is not one; the current channel is nearly as straight as it was in 1918 (Table 7, Figure 16). However, the active channel width parameter has decreased from an estimated 1,700 ft to 460 ft, a 75% reduction in 80 years (Riparian Boundary Results, Table 7, Figure 17).

Results from the HEC-RAS model show that since 1962 the channel dimensions have changed from a wide shallow channel to a narrow, deep channel. Although total wetted width (a combination of the width of the main channel and the estimated width of over bank flooding for each cross section) has decreased over time, the amount of over bank flooding has decreased more rapidly than the narrowing of the channel (HEC-RAS Results, Table 7). The amount of over bank flooding has decreased from approximately 30% of the total width to 10% (Figure 18). While width has decreased, the estimated average channel depth has doubled since 1962 (HEC-

RAS Results, Table 7). As a result, the width to depth ratio (channel width divided by average depth) has decreased almost 4-fold since 1962. Channel area estimates show a general decrease between 1962 and 1999, however the decreasing trend is not consistent. The wetted perimeter values, however, steadily declined to a value approximately half of the 1962 estimate for perimeter. Combined with the channel area data, the decreasing trend in wetted perimeter indicates that although water conveyance may have decreased slightly since 1962, the more significant change is in the form of the channel such that a flow of 5,000 cfs is interacting with less bank and bed surface area in 1999 than in 1962. As a consequence of a smaller, deeper channel, the HEC-RAS model estimates that the average velocity has increased. Along with the changes in the physical shape of the channel, the elevation of the channel bed has continuously decreased since 1962. Although a significant amount of bed degradation occurred between 1972 and 1992, the fastest rate of elevation lowering occurred between 1992 and 1997. The mean channel bed slope has also steadily decreased since 1962.

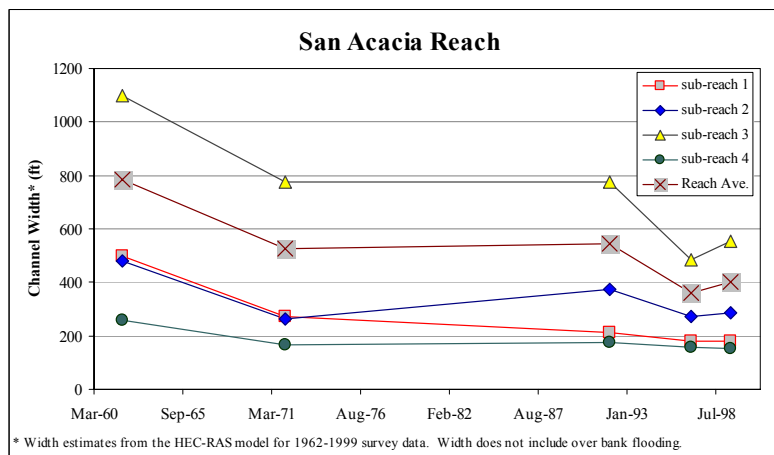
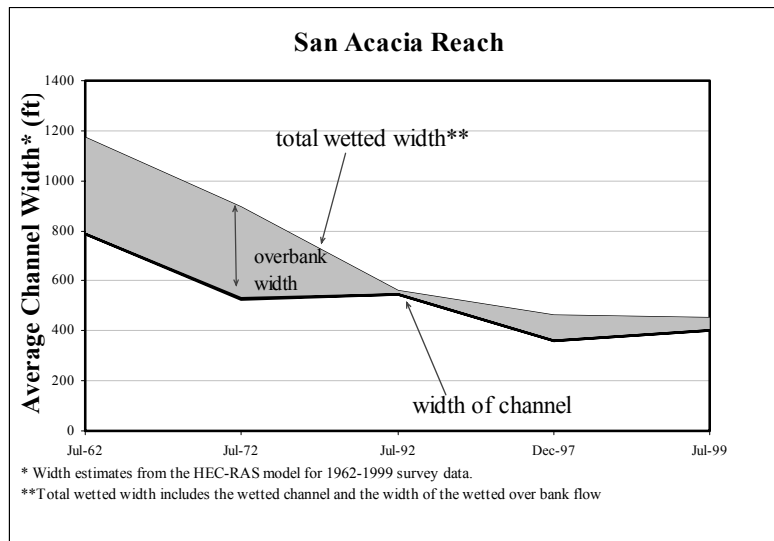


Figure 18: Channel widths and overbanking since 1962, Rio Grande – San Acacia reach.

Results from the STARS model indicate that for an increasing flow, channel width, depth, area and velocity on average increase. The channel parameters as estimated by the STARS model at 5,000 cfs have similar values to those estimated by the HEC-RAS model (Table 7).

Table 7: Summary of reach average values for the San Acacia reach as estimated from riparian boundaries on the historic photographs, and by the HEC-RAS and STARS models.

RIPARIAN BOUNDARY RESULTS	1918	1935	1949	1962	1972	1985	1992
Active Channel Width (ft)	1,700	1,640	1,300	740	530	580	460
Channel Sinuosity (ft/ft)	1.15	1.30	1.11	1.06	1.05	1.04	1.05

HEC-RAS RESULTS	1962	1972	1992	1997	1999	Rate of Change (1962-1999)
Total Wetted Width (ft) (includes overbank width)	1,170	900	560	460	460	-9.7 ft/yr
Width of Channel (ft)	790	530	540	360	400	-8.2 ft/yr
Maximum Depth (ft)	5.0	6.4	5.4	6.9	6.7	1.0 in/yr
Average Depth (ft)	2.1	2.5	3.8	4.1	4.1	1.0 in/yr
Width/Depth Ratio (ft/ft)	380	210	140	90	100	-
Channel Area (sq. ft)	1,620	1,330	1,610	1,340	1,380	-10.1 sq. ft/yr
Wetted Perimeter (ft)	814	532	550	364	404	-8.2 ft/yr
Average Velocity (ft/sec)	3.7	4.7	4.0	4.4	4.3	0.02 ft/sec/yr
Mean Bed Elevation (ft)	4639.5	4639.0	4633.9	4631.2	4630.4	-3 in/yr
Mean Bed Slope (ft/ft)	0.00091	0.00085	0.00086	0.00081	0.00080	-

STARS RESULTS	Flows (cfs)						
	200	500	1000	2000	3000	5000	7000
Wet Channel Width (ft)	170	220	280	350	400	450	480
Average Depth (ft)	1.0	1.4	1.9	2.6	3.2	4.1	4.9
Channel Area (sq. ft)	170	280	440	700	930	1,340	1,730
Average Velocity (ft/sec)	1.8	2.2	2.7	3.3	3.7	4.4	4.9

4.4.2 Sub-Reach 1 Conditions

Although sub-reach 1 has been a relatively narrow channel since the 1918 records (as compared to the other sub-reaches), it has still narrowed, deepened and incised. The riparian boundary data (Table 8) indicates that channel width in 1992 was only 33% of its 1918 width. Width estimates from HEC-RAS model results indicate that the channel has narrowed at approximately 10 feet per year since 1962. The STARS model results show that although width increases with increasing flows, it is only a small increase. Results from the HEC-RAS model predict only 10 feet of over bank flooding at 5,000 cfs in the 1999 data set thus indicating that almost all the flow stays in the main channel even at a channel forming discharge. With width decreasing and depth increasing, the width to depth ratio has decreased from about 140 to 30 between 1962 and 1999. The wetted perimeter estimates have decreased by 65% since 1962, while the channel area has decreased by only 30%, indicating that the dimensions of the channel are changing. According to the mean bed elevation data in Table 8, degradation between 1962 and 1999 was approximately 4.3 in/yr or 13.3 feet total.

Table 8: Summary of sub-reach 1 average values for the San Acacia reach as estimated from riparian boundaries on the historic photographs, and by the HEC-RAS and STARS models.

RIPARIAN BOUNDARY RESULTS	1918	1935	1949	1962	1972	1985	1992
Active Channel Width (ft)	570	570	650	380	230	200	190
Channel Sinuosity (ft/ft)	1.01	1.05	1.03	1.05	1.04	1.01	1.01

HEC-RAS RESULTS	1962	1972	1992	1997	1999	Rate of Change (1962-1999)
Total Wetted Width (ft) (includes overbank width)	570	350	220	190	190	-9.7 ft/yr
Width of Channel (ft)	500	270	210	180	180	-8.2 ft/yr
Maximum Depth (ft)	5.9	8.8	7.2	9.1	9.5	1.0 in/yr
Average Depth (ft)	3.7	4.5	5.8	6.3	6.6	1.0 in/yr
Width/Depth Ratio (ft/ft)	140	60	40	30	30	-
Channel Area (sq. ft)	1,660	1,420	1,270	1,170	1,200	-10.1 sq. ft/yr
Wetted Perimeter (ft)	500	280	220	190	180	-8.2 ft/yr
Average Velocity (ft/sec)	3.5	3.8	4.1	4.5	4.3	0.02 ft/sec/yr
Mean Bed Elevation (ft)	4661.3	4658.2	4653.3	4648.8	4648.0	-3 in/yr
Mean Bed Slope (ft/ft)	0.00072	0.00053	0.00065	0.00077	0.00084	-

STARS RESULTS	Flows (cfs)						
	200	500	1000	2000	3000	5000	7000
Wet Channel Width (ft)	110	120	130	150	160	170	190
Average Depth (ft)	1.8	2.1	2.8	3.8	4.6	5.8	7.0
Channel Area (sq. ft)	210	260	370	550	720	990	1,280
Average Velocity (ft/sec)	1.5	2.3	3.1	4.0	4.5	5.4	5.9

4.4.3 Sub-Reach 2 Conditions

Like sub-reach 1, sub-reach 2 has become narrower, and deeper, however, unlike sub-reach 1, the channel area has increased slightly. Channel width and over bank flooding has decreased continuously since 1962. In the 1962 data, over bank flooding doubled the width of the wetted channel (HEC-RAS Results, Table 9), whereas model results indicate that there is no over bank flows by 1999. The disappearance of over bank flooding is coincident with an increase in channel area, indicating that the channel dimensions changed to accommodate the entire flow. This variation in physical parameters is also coincident with a change in channel morphology to a meandering channel form.

As in sub-reach 1, the channel bed in sub-reach 2 has degraded, however data indicate that sub-reach 2 degraded an average of 11.5 feet, 1.8 feet less than sub-reach 1 between 1962 and 1999 (HEC-RAS Results, Table 9). Elevation data indicate that the highest rates of incision occurred in the 1990's, however, the average bed slopes did not decrease consistently over the period of record.

Table 9: Summary of sub-reach 2 average values for the San Acacia reach as estimated from riparian boundaries on the historic photographs, and by the HEC-RAS and STARS models.

RIPARIAN BOUNDARY RESULTS	1918	1935	1949	1962	1972	1985	1992
Active Channel Width (ft)	1,290	1,270	1,420	550	230	320	270
Channel Sinuosity (ft/ft)	1.03	1.47	1.08	1.02	1.01	1.02	1.05

HEC-RAS RESULTS	1962	1972	1992	1997	1999	Rate of Change (1962-1999)
Total Wetted Width (ft) (includes overbank width)	910	530	400	290	290	-15.5 ft/yr
Width of Channel (ft)	480	260	370	270	290	-5.5 ft/yr
Maximum Depth (ft)	4.6	6.1	6.2	7.9	7.4	0.8 in/yr
Average Depth (ft)	2.1	2.5	4.4	4.8	5.1	0.8 in/yr
Width/Depth Ratio (ft/ft)	230	100	85	55	55	-
Channel Area (sq. ft)	1,330	890	1,630	1,397	1,436	1.8 sq.ft/yr
Wetted Perimeter (ft)	600	260	380	280	290	-8.8 ft/yr
Average Velocity (ft/sec)	4.0	7.5	3.6	3.8	3.9	No change
Mean Bed Elevation (ft)	4653.3	4652.1	4646.4	4643.8	4641.8	-3 in/yr
Mean Bed Slope (ft/ft)	0.00066	0.00050	0.00091	0.00076	0.00070	-

STARS RESULTS	Flows (cfs)						
	200	500	1000	2000	3000	5000	7000
Wet Channel Width (ft)	170	190	200	240	260	280	300
Average Depth (ft)	1.0	1.3	1.9	2.7	3.4	4.8	5.9
Channel Area (sq. ft)	170	250	400	630	870	1,310	1,740
Average Velocity (ft/sec)	1.8	2.5	3.0	3.7	4.0	4.5	4.7

4.4.4 Sub-Reach 3 Conditions

Although this sub-reach has always been the widest and shallowest of the sub-reaches, changes in its channel dimensions have similar patterns to those found in the other sub-reaches. The average active channel was estimated to be almost 2,400 feet in 1918 (Riparian Boundary Results, Table 10), while the next widest reach, sub-reach 2 was only 1,300 feet wide. Although the widest, the rate of width decrease since 1962 is the greatest among the sub-reaches at 21 ft/yr (HEC-RAS Results, Table 10). The amount of total width contributed by over bank flows has also decreased from almost 400 feet in 1962 to 100 feet in 1999. The STARS model results show that the width of the channel at low flows (200 to 500 cfs) is comparable to those estimated in sub-reach 1 and 2, but that as the flow increases, the width increases at a steady rate. Sub-reach 3 is also the shallowest of the sub-reaches, estimated at an average of 1.5 feet in 1962 and 2.8 feet in 1999 data. Channel area and wetted perimeter values in 1999 are both less than found in the 1962 data.

As in other sub-reaches, the bed elevation data indicate that the channel bed in sub-reach 3 has degraded since 1962. However, the degradation found in sub-reach 3 is only 7.5 feet or a rate of 2.4 inches per year. Sub-reaches 1 and 2 had higher degradation rates at 3 inches per year, which may indicate that the rate of degradation decreases downstream. Unlike sub-reaches 1 and 2, the channel slope almost continuously decreased since 1962.

Table 10: Summary of sub-reach 3 average values for the San Acacia reach as estimated from riparian boundaries on the historic photographs, and by the HEC-RAS and STARS models.

RIPARIAN BOUNDARY RESULTS	1918	1935	1949	1962	1972	1985	1992
Active Channel Width (ft)	2,380	2,340	1,650	1,160	1,070	870	680
Channel Sinuosity (ft/ft)	1.19	1.26	1.10	1.10	1.08	1.08	1.09

HEC-RAS RESULTS	1962	1972	1992	1997	1999	Rate of Change (1962-1999)
Total Wetted Width (ft) (includes overbank width)	1,470	1,120	800	670	650	-20.8 ft/yr
Width of Channel (ft)	1,100	780	780	490	550	-15.9 ft/yr
Maximum Depth (ft)	4.7	6.0	4.2	5.7	5.5	0.2 in/yr
Average Depth (ft)	1.5	1.9	2.6	2.8	2.8	0.4in/yr
Width/Depth Ratio (ft/ft)	730	410	300	180	200	-
Channel Area (sq. ft)	1,890	1,600	1,810	1,450	1,510	-11.9 sq.ft/yr
Wetted Perimeter (ft)	1,100	780	780	490	560	-15.9 ft/yr
Average Velocity (ft/sec)	3.5	3.7	4.0	4.3	4.0	0.02 ft/sec/yr
Mean Bed Elevation (ft)	4635.1	4635.1	4630.2	4628.1	4627.6	-2.4 in/yr
Mean Bed Slope (ft/ft)	0.00093	0.00095	0.00082	0.00071	0.00073	-

STARS RESULTS	Flows (cfs)						
	200	500	1000	2000	3000	5000	7000
Wet Channel Width (ft)	210	280	370	490	570	660	700
Average Depth (ft)	0.8	1.1	1.4	1.8	2.1	2.6	3.1
Channel Area (sq. ft)	160	300	470	770	1,030	1,490	1,940
Average Velocity (ft/sec)	1.8	2.2	2.6	3.1	3.4	4.1	4.6

4.4.5 Sub-Reach 4 Conditions

Just prior to the 1962 data collection effort, sub-reach 4 was straightened and narrowed considerably, which accounts for the large change in channel width and sinuosity between 1949 and 1962 (Riparian Boundary Results, Table 11). Due to shallow average depth and narrow width, the channel was not sufficient to convey the channel forming discharge until after 1972. By 1992, although the width of the channel remained similar to that of the originally constructed channel, the average depth had more than doubled (HEC-RAS Results, Table 11). Width and depth results from the STARS (Table 11) model indicate that depth increases with discharge, but that width does not. The channel area has not changed significantly since 1962, nor has the wetted perimeter since 1972.

The elevation of this sub-reach has decreased by almost 8 ft, which is less degradation than found in sub-reaches 1 and 2, but more than in sub-reach 3. As with the other sub-reaches, the highest rates of erosion occurred between 1992-1997. Mean bed slope has not changed significantly since 1962.

Table 11: Summary of sub-reach 4 average values for the San Acacia reach as estimated from riparian boundaries on the historic photographs, and by the HEC-RAS and STARS models.

RIPARIAN BOUNDARY RESULTS	1918	1935	1949	1962	1972	1985	1992
Active Channel Width (ft)	660	730	650	200	160	190	170
Channel Sinuosity (ft/ft)	1.29	1.36	1.25	1.00	1.00	1.00	1.00

HEC-RAS RESULTS	1962	1972	1992	1997	1999	Rate of Change (1962-1999)
Total Wetted Width (ft) (includes overbank width)	950	1,050	180	160	150	-21.4 ft/yr
Width of Channel (ft)	260	170	180	160	150	-2.7 ft/yr
Maximum Depth (ft)	5.8	6.4	7.1	7.6	7.7	0.7 in/yr
Average Depth (ft)	3.0	2.8	5.8	5.9	5.5	1.0 in/yr
Width/Depth Ratio (ft/ft)	90	60	30	30	30	-
Channel Area (sq. ft)	970	830	1,030	920	850	-0.12 sq. ft/yr
Wetted Perimeter (ft)	260	170	180	160	160	-2.6 ft/yr
Average Velocity (ft/sec)	4.7	5.3	5.1	5.7	6.2	0.02 ft/sec/yr
Mean Bed Elevation (ft)	4615.7	4616.4	4610.7	4607.7	4607.8	-2.5 in/yr
Mean Bed Slope (ft/ft)	0.0011	0.00087	0.0011	0.0018	0.0014	-

STARS RESULTS	Flows (cfs)						
	200	500	1000	2000	3000	5000	7000
Wet Channel Width (ft)	100	130	150	150	150	160	170
Average Depth (ft)	1.3	2.2	3.3	4.7	5.7	7.1	8.0
Channel Area (sq. ft)	130	280	440	660	830	1,100	1,340
Average Velocity (ft/sec)	1.8	2.1	2.5	3.1	3.7	4.8	5.6

4.5 Bed Material - Sediment Characteristics

Two distinct bed material sizes, sand and gravel, are present in the study area, which usually forms two distinct layers in the first 4 miles of the reach (through subreaches 1, 2 and part of 3). The sand layer is active during most flows (>300 cfs) and overlies the gravel layer,

which appears to be active only during flows that approach channel forming. Surface sampling at the San Acacia gage (1966-1999) and throughout the reach (1995-1999) have measured exposed patches of gravel, but most commonly the overlying sand layer was sampled. In May 2000, the gravel layer was explicitly sampled for: 1) grain size distribution, 2) continuity across each cross section line, 3) continuity along the channel throughout the study area and 4) depth buried by the overlying sand layer.

Measurements at the San Acacia gage indicate that surface bed material was sand-sized, 0.07 to 1.0 mm, from 1966 to approximately 1988; however after 1988 gravel-sized material, up to 51 mm, were present in the surface bed material samples (Figure 19). Grain size data separated by month, indicates that the largest grain sizes were consistently measured from March through July (Figure 20), while the smallest grain sizes were measured between December and February. In fact, gravel has not been measured during the winter months to date, indicating that it is buried by sand during this period. This seasonal trend likely reflects erosion of the sand layer during spring and early summer due to the ‘sediment-free’ dam releases of spring runoff and deposition during the ‘sediment-laden’ arroyo fed flows of summer.

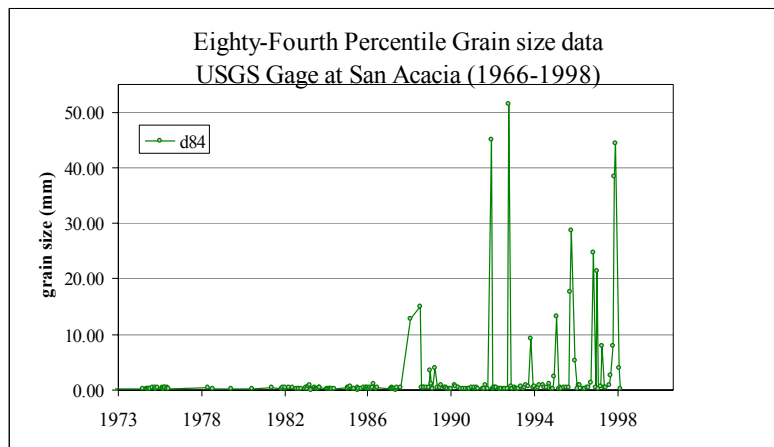


Figure 19: Bed Material Measurements at the USGS Rio Grande gage, San Acacia.

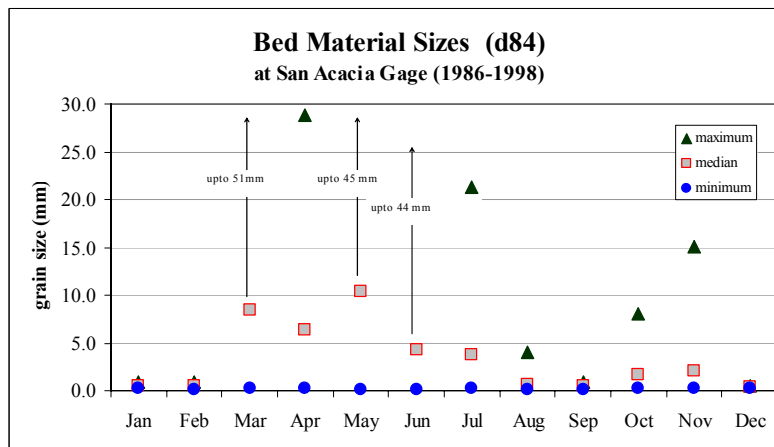


Figure 20: Monthly variability in grain sizes at the USGS Rio Grande gage, San Acacia.

Bed material samples collected throughout the reach between 1995 and 1999 (Table 12) found that although gravel sized particles were consistently sampled in sub-reaches 1 and 2, sand-sized particles dominated sub-reaches 3 and 4. For sub-reaches 3 and 4, limited surficial gravel was sampled during this time period.

Table 12: Grain sizes (d_{84}) throughout the San Acacia reach. Grain sizes are in millimeters.

	May-95	Dec-97	Jul-99	Oct-99
sub-reach 1	47.03	12.06	3.76	12.10
sub-reach 2	17.20	1.64	3.37	1.13
sub-reach 3	1.56	0.38	1.33	0.86
sub-reach 4	0.42		1.02	0.57
reach average	10.81	2.31	2.01	2.45

In May 2000, a data collection effort aimed at assessing the gravel layer throughout the reach found that: 1) the gravel layer contained larger sediment sizes than found at the gaging station or from earlier surface sampling efforts (Figure 12), and 2) the gravel layer was continuous throughout sub-reaches 1 and 2, and dis-continuous in sub-reaches 3 and 4. Thirty-nine sample locations (cross sections) exist in this study reach, which have been sampled throughout the 1990s and in 2000. Field observations were taken between these cross sections for determining the extent of the gravel layer. Bed material data were collected using the Wolman pebble count methodology (Leopold, Wolman, and Miller, 1964) in locations in which the gravel layer was exposed or by ‘grab’ samples for those areas in which the gravel was buried beneath the sand. These ‘grab’ samples were collected by removing the sand cover, then collecting 3-4 shovels of sediment, which were later wet sieved. The median grain size (d_{50}), the eighty-fourth grain size (d_{84}) and the thirty-fifth grain size (d_{35}) were determined using the particle size distributions for each sample. No gravel present was recorded when the sand layer was greater than 6 feet (~2 meters).

The median grain sizes ranged from 6 to 73 mm in the study area. Although the largest measured particles (73 mm or cobble size) were found in sub-reach 3, coarse gravel to very coarse gravel (32-64 mm sizes) were sampled throughout both sub-reaches 2 and 3. A systematic decrease in particle sizes does not exist in the downstream direction (Figure 21) likely due to local sources of gravel such as Arroyo Alamillo or Arroyo de la Parida (Figure 11).

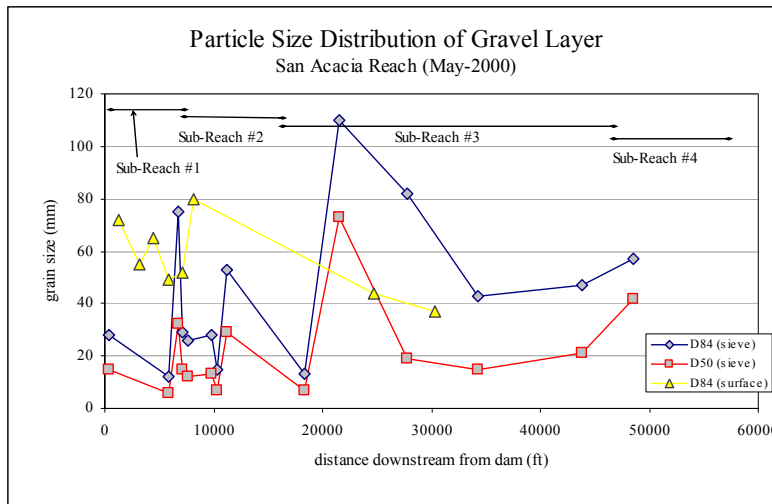


Figure 21: Particle size distribution of gravel layer, Rio Grande – San Acacia Reach.

By probing through the sand layer to the gravel in each of the 39 cross sections and between these cross sections, a continuous gravel layer was found throughout sub-reaches 1 and 2. Although present in sub-reaches 3 and 4, the gravel did not form a complete and continuous layer. Field observations of the exposed gravel surfaces in sub-reaches 1 and 2 also indicate that it has formed an ‘armored’ surface. An ‘armored’ surface indicates that the gravel layer has experienced differential sediment transport, where the finer particle sizes were selectively transported away, leaving a coarse layer of particles. This armored surface is more resistant to sediment transport than the original deposit and may act to ‘protect’ the channel bed from scour during smaller floods.

The depth to gravel or depth of the active sand layer measurements found that the sand layer was thickest in sub-reaches 3 and 4 (Table 13). Sand layer depth measurements were taken every 10-12 feet at each of the 39 cross sections. These measurements were width integrated for an average cross section depth. Also, a weighted average, based on channel length between cross sections, was calculated for each sub-reach. Sub-reaches 1 and 2 have the least amount of sand overlying the gravel, ~2 ft, while sub-reaches 3 and 4 have over 3 feet of sand.

Table 13: Summary of gravel layer characteristics by sub-reach.

	Median grain size (mm)	Depth to gravel (feet)	Spatially continuous?
sub-reach 1	28	1.8	yes
sub-reach 2	24	2.2	yes
sub-reach 3	48	3.5	no
sub-reach 4	no data	3.2	no

4.6 Sand Load from Upstream Sources

The sediment load, sand sized particles, passing the San Acacia gage at a discharge of 5,000 cfs was estimated to be 12,700 and 158,100 tons/day for spring and summer flows, respectively. Total bed loads of sand sized particles were estimated using a revised Modified Einstein procedure (Colby and Hembree, 1955; USBR, 1966) through the computer program *Psands* (USBR, 1969). Utilizing *Psands* and data collected between 1990-1999, which represents the current sediment and water relationship (Figure 9), the current sand load was estimated. These data were divided into spring runoff flows, summer (thunderstorm) flows and fall-winter flows, since distinct sediment concentration characteristics exist between these seasons. An initial inspection of fall-winter flows indicated that although sand-sized sediment is transported during these seasons, transport of sand in the spring and summer seasons dominate the sediment transport estimates. Data from 18 spring flows and 12 summer flows were available for analysis. Fitting a linear regressed equation in Log-Log space to each data set found that for the channel forming flow, 5,000 cfs, approximately 12,700 and 158,200 tons per day of sand-sized sediment were transported for the spring and summer flows, respectively (Figure 22). These data support other data indicating that the summer flows which are produced by storm runoff in arroyos, carry an estimated order of magnitude more sand sized particles than the spring flows released from Cochiti reservoir.

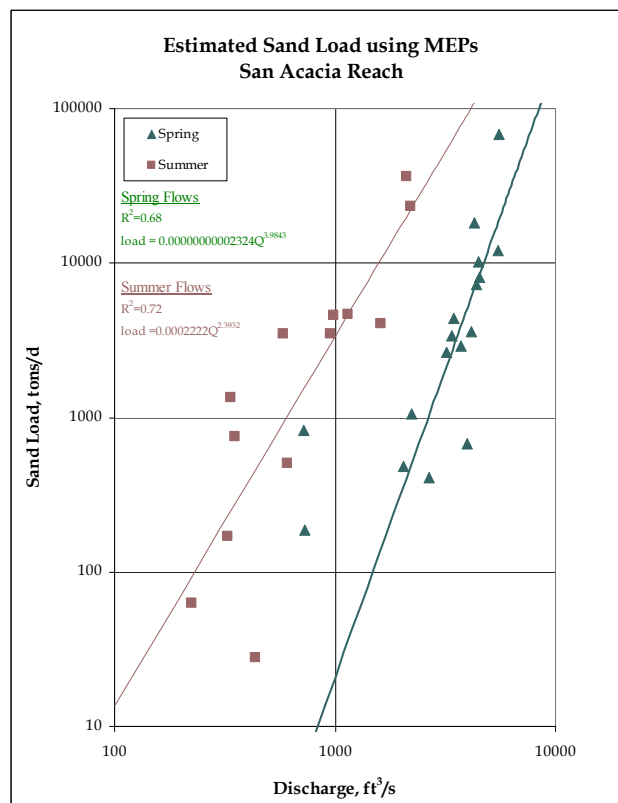


Figure 22: Estimated sand load results from the modified Einstein procedure, Rio Grande gage at San Acacia.

4.7 Sand Load from the River Channel

Historic (1962) and current (1992, and 1999) cross section data comparisons found that the highest rates of channel bed erosion occurred in sub-reach 3, between 1992-1999 (Table 14). Comparing the volume change between cross sections in the program, *Scour and Fill* version 7.1 (USBR, 1995), the total volume removed was estimated for each cross section. Using weighted averages, rates of volume change were estimated (Table 14). These data indicate that degradation occurred at a rate faster in the 1990's than from the 1962 to 1992 period of record.

Table 14: Volume of sediment removed by bed lowering (degradation) for each sub-reach in the San Acacia reach, as determined by cross section comparisons.

	1962-1992 (yd ³ /yr)	1992-1999 (yd ³ /yr)
sub-reach 1	14,000	31,000
sub-reach 2	38,000	76,000
sub-reach 3	96,000	186,000
sub-reach 4	10,000	19,000
Entire Reach	158,000	312,000

4.8 Sediment Routing

While accounting for external and internal sediment sources, a sediment routing model that compares transport capacity to sediment supply for predicting sand erosion, revealed two main results: 1) scour of the current sand layer could occur within 6 months for transport zones 1 and 2, but would require approximately 3 years for the wide zones (transport zones 6 and 7); and 2) sediment supply for zones 1 and 2 is dominated by external (upstream) sediment sources, while in-stream sediment supplies, such as an eroding channel bed in the previous zone, significantly increased the sediment supply in the remaining transport zones. The San Acacia reach was divided into 8 sections or transport zones (Figure 23), to more precisely describe variations in slope, a major variable in the sediment transport equations and other channel characteristics. These zones generally reflect the sub-reaches (Table 15), however the transport zones do not always have the same boundaries as the sub-reaches, and some sub-reaches are represented by multiple transport zones (Table 15). Therefore, values of channel parameters for each zone, such as width or depth (Table 16), do not necessarily correspond to the sub-reach values. These eight transport zones were used for the sediment transport modeling and bed stability analysis.

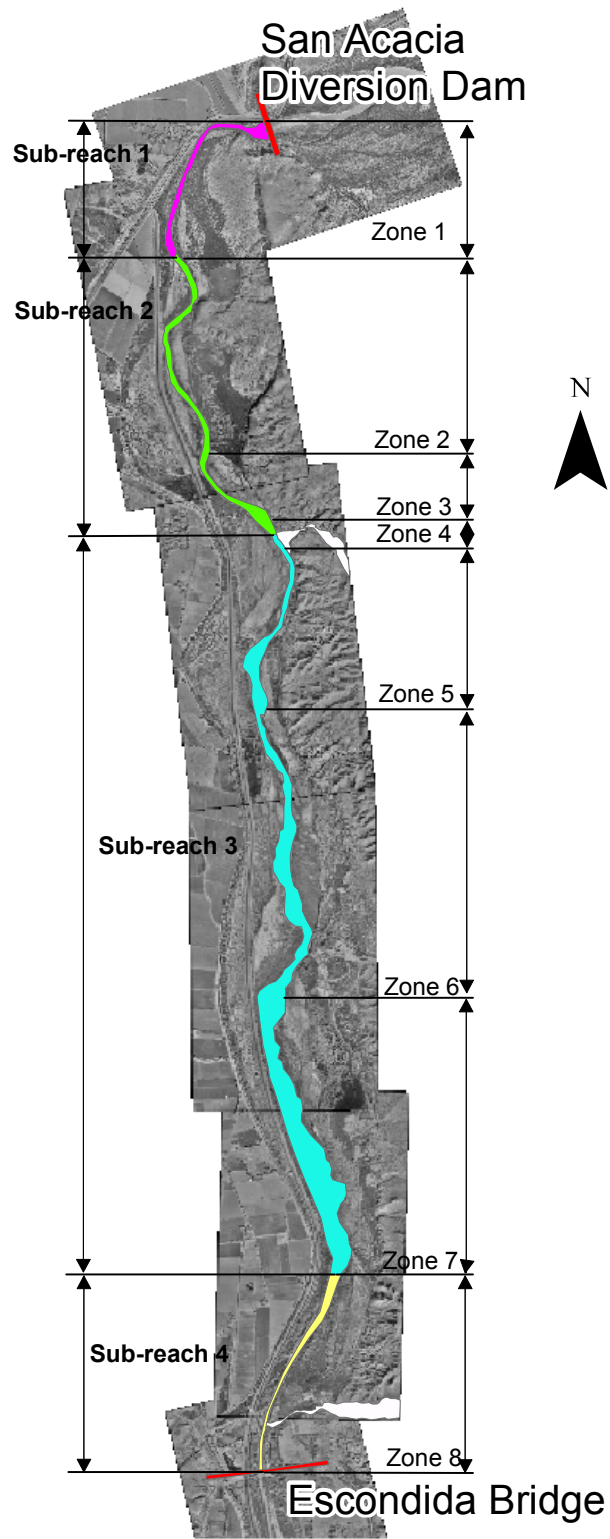


Figure 23: Sediment transport zone locations, Rio Grande – San Acacia Reach.

Table 15: Summary of Sediment Transport Zones, San Acacia Reach.

Sub-Reach	Transport Zone	Cross Sections	Description
1	1	SA1209-SA1223	deeply incised and narrow, medium to coarse gravel
2	2	SA1223-SA1232	slightly sinuous, slightly wider than zone 1, medium to coarse gravel
2	3	SA1232-SA1243	less steep than zone 2, fine to medium gravel
3	4	SA1243-SA1246	steepest zone, cobbles and boulders
3	5	SA1246-SA1256	transitional zone, coarse gravel
3	6	SA1256-SA1280	straight and wider than the previous zones, very coarse gravel
3	7	SA1280-SA1302	widest zone, coarse gravel
4	8	SA1302-SA1314	deep and narrow, no gravel samples collected

Table 16: Current Conditions of Channel Parameters for each Transport Zone, San Acacia Reach.

Transport Zone	Width (ft)	Depth (ft)	Velocity (ft/sec)	Gravel-d50 (mm)	Gravel-d84 (mm)	WS* Slope (ft/ft)	Thalweg Slope (ft/ft)
1	180	5.7	4.8	17	51	0.00086	0.00059
2	230	5.7	4.5	14	41	0.00076	0.00078
3	280	4.6	3.7	7	13	0.00074	0.00102
4	280	4.5	6.1	14	93	0.00119	0.00035
5	230	5.9	2.9	30	92	0.00041	0.00028
6	410	4.3	3.2	13	42	0.00101	0.00103
7	730	3.4	2.2	20	51	0.00092	0.00108
8	150	6.9	5.3	N/A	N/A	0.00048	0.00020

*Water Surface is abbreviated as WS.

Based on the Yang (1972) model, which estimates the discharge dependent transport capacity, sediment was routed through the entire reach while conserving mass for 4 different hydrographs. The incoming water discharge for the reach was determined from the average daily discharges from hydrographs in the 1990's. Hydrographs usually covered a one year period; however, one model covered a five year period. Four sets of discharge data were used in

this exercise: 1) a wet year - the 1994 hydrograph; 2) a dry year - the 1996 hydrograph; 3) an average of all 1990's hydrograph for the 'average year'; and 4) hydrographs from 1990 to 1995 for a multiple year run. The model was also tested for low discharges (<200 cfs) sensitivities since several days in the data did not have any discharge (e.g., the river was dry); results from this test indicated that the model produced reasonable results and therefore was not sensitive to low water discharges. Thus, no low flow adjustments were necessary for the discharge data used in the model.

The sediment load for this model was limited to the sand load. The sediment load entering the first zone of the reach was estimated for each day using the sand load results from the *PSANDS* model (described in Section 4.6) at the San Acacia gage. For the downstream zones, sediment load was determined as the outgoing sediment load for the zone immediately upstream. The model considered the amount of sand input to each zone, calculated the potential volume of in-zone degradation or scour of the sand layer, and then determined the amount of sediment leaving each zone. In-zone scour was determined by comparing the estimated transport capacity of each zone to the amount of in-coming sediment; when capacity was lower than the incoming sand load, sediment was deposited equally throughout the zone and a new depth of the sand layer was determined. However, when capacity was greater than incoming sediment load, and sediment was available for scour, sediment was uniformly removed throughout the reach until sediment supply equaled transport capacity, then a new depth of the sand layer was calculated. The amount of scoured sediment was added to the output, which became the input sediment for the next zone downstream. The depth of scour was limited to the depth of the gravel layer, therefore once the gravel layer was reached, no additional scour could occur in that zone. The amount of sediment routed was conserved and recorded. Sand depth in each zone was also recorded for each run. Channel dimensions (width, depth, etc) for each zone were determined through the HEC-RAS model using the current (1999) cross section data.

Model results from the wet-year's hydrograph (1994) indicate that the sand layer would scour significantly. The 1994 hydrograph had peak flows over 6,000 cfs in May, with the average spring runoff around 4,000 cfs (Figure 24). The spring runoff period extended from mid April through June, while the summer flow from thunderstorm events occurred in August and September, but only one of these events peaked over 3,000 cfs. The spring and winter flows both scour the sand layer. While there was some deposition predicted during the summer flows, the deposits would be quickly scoured during the winter flows.

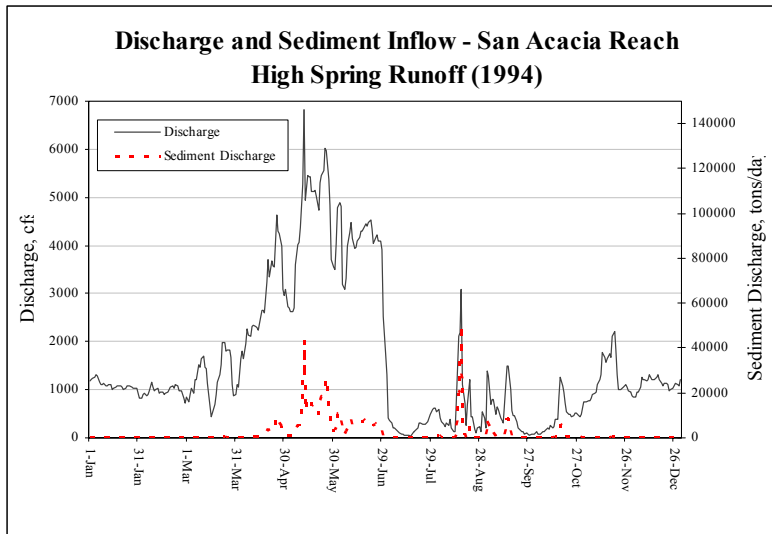


Figure 24: USGS Rio Grande gage (at San Acacia) discharge data for a wet year (1994) and the corresponding sediment discharge.

For the dry-year's hydrograph (1996) with a strong summer storm season, the model indicates that a single thunderstorm induced flow would deposit several feet of sediment that will last for several months before erosion occurred from the winter flows. Data from the 1996 year (Figure 25) contains no spring runoff, and only minor flows during the summer, except one large flow at the end of June that peaked just over 5,000 cfs. Winter flows averaged about 1,000 cfs. Model results indicate that several feet of sand sized sediment deposited in the first zone. As this sediment was slowly transported out of zone 1, it deposited in zone 2 before continuing to move downstream.

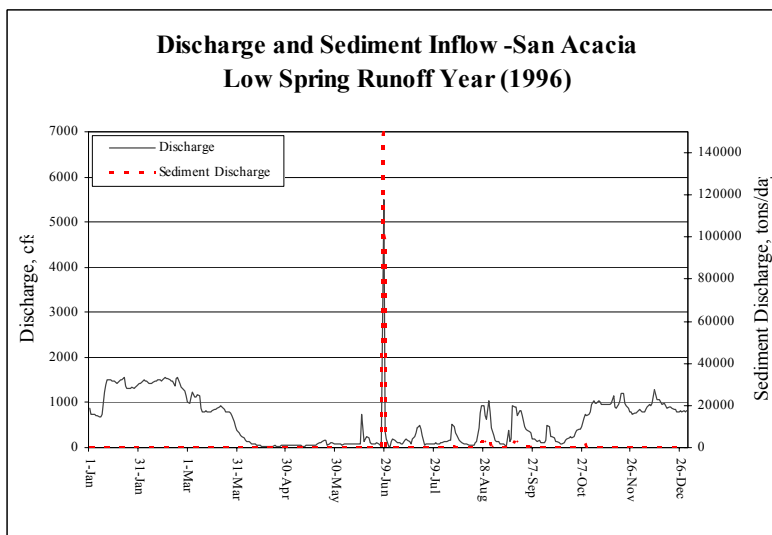


Figure 25: USGS Rio Grande gage (at San Acacia) discharge data for a dry year (1996) and the corresponding sediment discharge.

Using the average-year hydrograph, the model indicated that winter flows and spring runoff could easily transport the sand layer completely away. The average hydrograph has winter flows ranging from 1,000 to 1,500 cfs, spring flows up to almost 3,500 cfs, and summer flows from 500 to 1,000 cfs. According to the model, the winter flows are sufficient to scour sand sized sediment in most zones, and that significant scour occurs in all zones during spring runoff. Although the summer flows are modest, some zones show deposition during this period. However, this deposition is limited to zones with low slopes, and even in these zones, the deposition is temporary.

For the multiple year hydrograph, model results show that while sediment laden summer flows cause in-channel deposition, spring and winter flows consistently scour sediment in each zone, and that the amount of scour always exceeds the amount of summer deposition. The five year hydrograph begins in 1990 which is a dry year (with little spring runoff), while the subsequent years all have significant spring runoff flows (Figure 26). Winter flows vary throughout the five years, but most years have periods in which the flows are near 1,000 cfs. In 1991, several summer runoff events produced large amount of sediment deposition, while smaller events in 1993 and 1994 produced smaller deposits. Model results indicate that these summer deposits slowly propagate downstream during fall and winter flows but in zones 1 and 2, the sand layer erodes easily with both spring and winter flows. For zones 6 and 7, the current sand depth is predicted to be scoured to the gravel layer in approximately 3.5 and 2.5 years respectively if similar hydrographs of 1990-1995 occur in the next 5 years.

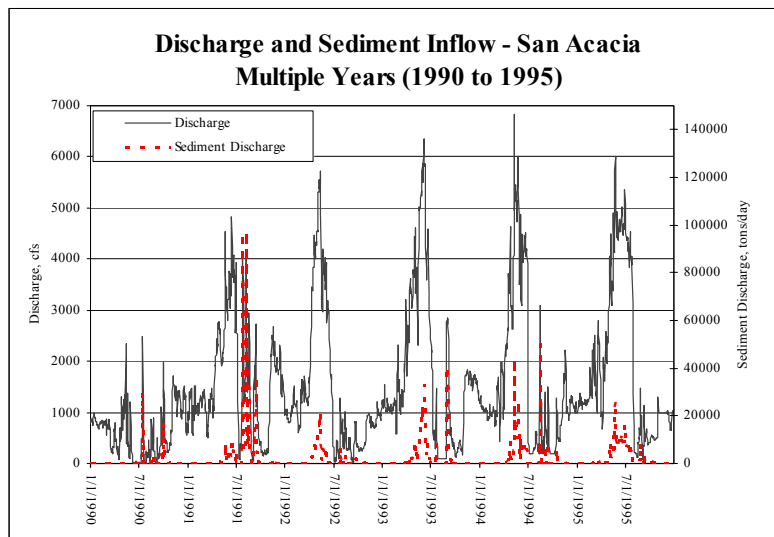


Figure 26: USGS Rio Grande gage (at San Acacia) discharge data for a 5-year period (1990-1995) and the corresponding sediment discharge.

5.0 EQUILIBRIUM SLOPE AND FUTURE CONDITIONS ASSESSMENT

A change in bed material size, continued narrowing, and channel bed incision all indicate that this channel is currently not stable, and that it will continue to evolve. For this study, channels described as ‘stable’ are those in which 1) the bed material is mobile during channel forming flows, but the sediment size is not changing, 2) supply of sediment is relatively steady, 3) general channel dimensions (e.g., width and depth) and slope are not changing significantly, and 4) the channel pattern remains constant over time. The systematic migration of a meander bend is still considered a stable channel even though the dimensions and location of the floodplain are constantly changing in this environment. This section assesses both the stability of the current slope and the measured grain sizes of the gravel layer. From this information, future conditions of channel pattern, slope and width were estimated. For purposes of this study, the equilibrium slope is defined and calculated using two methods: 1) the slope that transports the incoming sediment supply without any scour or fill on the channel bed, and 2) the slope required for the initiation of incipient motion of the current bed material.

5.1 Equilibrium Slope and Width Analysis

5.1.1 Historical Slopes

Current and historic channel slopes were determined using photometric and field measured cross section data in the HEC-RAS model. Results of this exercise show that slope has varied through time (Table 17), but that many transport zones now have slightly lower slopes or similar slopes to those from the 1960's.

Table 17: Summary of average water surface slopes from HEC-RAS at 5,000 cfs, San Acacia Reach (1962-1999).

Transport Zone	1962	1972	1992	1997	1999
1	0.00096	0.00089	0.00085	0.00074	0.00077
2	0.00107	0.00079	0.00107	0.00103	0.00092
3	0.00058	0.00043	0.00032	0.00031	0.00065
4	0.00109	0.00095	0.00125	0.00107	0.00093
5	0.00083	0.00090	0.00084	0.00067	0.00061
6	0.00080	0.00079	0.00078	0.00080	0.00091
7	0.00140	0.00146	0.00123	0.00133	0.00099
8	0.00101	0.00097	0.00064	0.00083	0.000700

5.1.2 Equilibrium Bed Slope based on Sediment Size

The channel bed slope stability analyses based on sediment size, found that the current channel slopes are close to equilibrium with the gravel-sized sediment, but not at equilibrium

with sand-sized sediment. Four sediment transport models, Schoklitsch (1932), Meyer-Peter & Muller (1948), Lane (1955), and Shields (1936), estimated ‘stable’ slopes based on channel conditions from the 1999 survey data. Schoklitsch’s model incorporates grain size and width with discharge to obtain the stable channel slope. The Meyer-Peter & Muller method combines discharge with bed roughness (Manning’s ‘n’ variable) and grain size, but also adds in channel depth. Lane’s model uses the critical tractive force along with channel depth to determine slope, while Shields’ model uses the Reynolds number with shear velocity and particle size. The analysis for the sand sizes was performed at a discharge of 3,000 cfs, since this is the estimated effective discharge, while a flow of 5,000 cfs, or bankfull discharge was used for the gravel data (Channel Forming Flow Section 4.2). Since zone 5 is transitional, stable slope estimates were not calculated. Slopes were not calculated for the gravel data in zone 8 either, since no gravel data was collected. Results for sand sized sediment (Table 18) show that the current channel slopes are all greater than the estimated stable slopes, while estimated slopes for gravel are similar to the current slopes. Hence, these data indicate that the sand layer is not stable with the current channel slope, but with the increase in sediment size to gravel, the current bed slopes are stable.

Table 18: Computed stable bed slopes for sand and gravel sized sediment for San Acacia reach.

Zone	Shoklitsch (1932)	MPM (1948)	Lane (1955)	Shields (1936)	Average of all Models	Water Surface Slope
Slopes for Sand Sized Particles						
1	0.00008	0.00024	0.00034	0.00002	0.00017	0.00077
2	0.00009	0.00040	0.00037	0.00002	0.00022	0.00092
3	0.00010	0.00041	0.00038	0.00002	0.00023	0.00065
4	0.00012	0.00049	0.00043	0.00002	0.00027	0.00093
5	N/A	N/A	N/A	N/A	N/A	N/A
6	0.00010	0.00043	0.00053	0.00003	0.00027	0.00091
7	0.00007	0.00033	0.00039	0.00002	0.00020	0.00099
8	0.00009	0.00041	0.00040	0.00002	0.00023	0.00070
Slopes for Gravel Sized Particles						
1	0.00121	0.00400	0.00073	0.00094	0.00172	0.00086
2	0.00128	0.00347	0.00059	0.00078	0.00153	0.00076
3	0.00089	0.00302	0.00039	0.00049	0.00120	0.00074
4	0.00140	0.00351	0.00068	0.00094	0.00163	0.00119
5	N/A	N/A	N/A	N/A	N/A	N/A
6	0.00182	0.00419	0.00056	0.00095	0.00188	0.00101
7	0.00388	0.00807	0.00148	0.00185	0.00382	0.00092
8	N/A	N/A	N/A	N/A	N/A	N/A

5.1.3 Estimated Equilibrium Slope and Width based on Sediment Supply

The equilibrium slope and width, estimated using a sediment analysis model indicated that the channel will generally continue to narrow and steepen. Sediment supply and current channel conditions were used in SAM (U.S. Army Corps of Engineers' SAM-Hydraulic Design Package for Channels, 1998), a model developed to estimate stream power and the associated channel characteristics such as width and Energy Grade slope (EG slope) based on supply of sediment. Energy grade slope is a combination of water surface slope with velocity head ($\text{velocity}^2/2 * \text{gravity}$). The sand load was estimated in Section 4.6 – Sand Load from Upstream Sources, at approximately 12,700 tons/day for a 5,000 cfs spring flow (Figure 22), while the current channel conditions are summarized in Table 16, Section 4.8 – Sediment Routing. Results from SAM include the estimated stable channel width and estimated stable Energy Grade Slope. The estimated stable channel width results indicate that most of the channel will continue to narrow (Table 19). With the exception of transport zones 6 and 7, the estimated stable EG slopes are generally steeper than the current EG slopes (Table 19). Zones 6 and 7 have EG slopes steeper than the estimated EG slopes from SAM. These results indicate that Zones 6 and 7 which still have channel features most similar to historic conditions have a significant potential to lose both energy (EG slope) and width, while the other zones will likely continue to only narrow.

Table 19: Computed stable width and EG slopes for the current channel conditions and sediment supply for flows of 5,000 cfs: San Acacia Reach.

Transport Zone	EG Slope (ft/ft)	Width (ft)		Est. Stable Width (ft)	Est. Stable EG Slope
1	0.00084	180		140	0.00098
2	0.00059	230		150	0.00096
3	0.00087	280		155	0.00089
4	0.00061	280		160	0.00091
5	0.00066	230		160	0.00091
6	0.00105	410		150	0.00081
7	0.00093	730		165	0.00075
8	0.00061	150		160	0.00085

5.1.4 Summary of Equilibrium Slopes and Widths from Sediment Transport Models

Bed slope analyses indicated that the current channel bed slopes are stable for the current channel that is gravel bedded, while the SAM analysis indicates that the channel will continue to narrow and increase in velocity to transport the current sand load. The historic slope data (Table 17) indicate that, in general, bed slopes have decreased since 1962, averaging about a 20% change. The stable bed slope assessments based on sediment size found that the current slopes

are close to equilibrium for the gravel-sized sediment. The predicted bed slopes for sand were significantly shallower than the current slopes, indicating that sand sized sediment is not the stable sediment size in this reach. Current channel conditions compared with the SAM results showed that only two zones had unstable EG slopes, while most zones would continue to narrow. Combining the bed slope analyses with the SAM results and historic trends indicates that although the bed slope is stable, the dimensions of the channel which have continuously changed over time will likely continue their trends toward a narrower, deeper channel with a faster velocity.

5.2 Stable Sediment Sizes

The gravel sizes measured in the first 4 miles (zones 1-4) downstream from San Acacia diversion dam are mobile when the flow approaches the channel forming discharge of 5,000 cfs (Table 20), however, the gravel sizes found in the remainder of the reach are not necessarily mobile at this flow. The flow needed to induce sediment mobility for the grains in the gravel layer was estimated using Yang's sediment transport model (1984) for gravel. Yang's model uses unit stream power to estimate sediment transport capacity. The measured d_{84} for each zone was used to represent the armored surface condition. Zone 5 is transitional, therefore no calculations were performed; also, no calculations were performed in zone 8 due to lack of data for the gravel layer.

Results from Yang's model indicated that grain sizes present in zones 1-4 are mobile near the channel forming discharge, but further downstream in zones 6-7, the current gravel sizes are not mobile. In zones 1 and 2, flows near 5,000 cfs, the channel forming/bankfull discharge, are estimated to transport the d_{84} particle size (Table 20). These data indicate that the gravel is stable for the current channel form in zones 1 & 2. Gravel in zones 3 and 4 can be transported with much lower flows, indicating that the current sediment sizes may not be stable, and that smaller flows can initiate sediment transport. In zones 6 and 7, the discharge necessary to initiate sediment transport is significantly higher than the channel forming discharge, indicating that the gravel currently present is not likely transported by the current hydraulic conditions in the river. The source of the gravels in zones 6 and 7 is likely from adjacent hillslopes, nearby arroyos and are relic fluvial deposits. Although the gravel measured in zones 1-3 may also be from these local sources, its systematic decrease in size suggests that it was likely transported from upstream sources.

Table 20: Grain sizes present, estimated sizes of grain mobile during a 5,000 cfs discharge and the specific discharge required to mobilize the current grains on the channel bed in the San Acacia Reach.

Transport Zone	Measured d_{84} Grain Size (mm)	Estimated Grain Size Mobile (mm)	Discharge for Grain Mobility (cfs)
1	51	32 to 64	4,800
2	41	16 to 32	5,600
3	13	16 to 32	3,700
4	93	32 to 64*	~3,000 for 64 mm*
5	91	not calculated	not calculated
6	41	8 to 16	22,500
7	56	2 to 4	greater than 35,000
8	none measured	not calculated	not calculated

*Yang’s model is not designed for grain sizes larger than 64 mm (very coarse gravel) therefore this model cannot accurately estimate the mobilizing discharge for the d_{84} present in zone 4.

5.3 Future Conditions - No Action Scenario

Data indicates that sub-reaches 1 and 2 have channel patterns and characteristics that are stable, while sub-reaches 3 and 4 have potential for continued channel evolution. The future conditions analysis focuses on three dominant channel features: 1) channel pattern, 2) bed material/grain size, 3) channel width and 4) channel bed elevation. Although each sub-reach is assessed individually, evolution in one sub-reach could affect the future condition results for another sub-reach, which will be summarized in the last section. The current sediment supply and discharge patterns are used in this assessment.

5.3.1 Future Conditions of Sub-Reach 1

Channel features such as channel patterns and grain sizes have not changed recently in sub-reach 1 and appear to be relatively stable. Sub-reach 1 is a straight channel with a gravel bed, intermittently covered by thin sand deposits. This channel is physically confined by railroad tracks and by tall terraces, and therefore cannot readily widen or flood. Although channel bed grain sizes could change in the future, the change from a sand bed to a gravel bed is complete. With a channel bed composed of gravel sized sediment, bed degradation is expected to decrease in the future, since the gravel bed is able to form armor layers resistant to erosion. Due to a decrease in incision, channel slope values are also expected to stabilize. Although the SAM analysis indicated that this sub-reach could still narrow, the historic analysis of channel width indicates width is stabilizing. In summary, significant changes in this sub-reach are not expected in the future.

5.3.2 Future Conditions of Sub-Reach 2

Although meandering channels, such as sub-reach 2, typically migrate across their floodplains, channel characteristics such as width, depth and slope should remain constant,

which is the trend expected for future conditions in sub-reach 2. Sub-reach 2 is a slightly meandering channel with a gravel bed that is intermittently covered by a thin layer of sand sized sediment. Unlike sub-reach 1, this channel is likely to slowly erode the confining banks (terraces and levee walls) and slowly migrate from its current location, due to its meandering channel pattern. However, channel characteristics such as width and depth are not expected to change significantly due to channel migration. Although the SAM results indicated a significantly narrower channel for the future, the current channel width appears to be stabilizing. As with sub-reach 1, the channel bed has already converted to gravel, which will likely inhibit future degradation, and hence stabilize channel slope. Although some conditions in sub-reach 2 may change, for example, specific channel location, the hydraulic properties of the channel are considered stable.

5.3.3 Future Conditions of Sub-Reach 3

The morphology of sub-reach 3 is expected to continue converting to a slightly meandering channel, which will be a channel that is narrower, deeper, and less steep. Current sub-reach 3 morphology conditions are: 1) zone 4 has already converted to slightly meandering channel, 2) zone 5 is in the process of converting, and 3) zones 6 and 7 are still dominated by a low-flow braided morphology, but prominent thalwegs have developed recently in portions of these zones. The development of a prominent thalweg may suggest that conversion to a single-threaded, meandering channel has already begun. Channel characteristics from sub-reach 2, an established meandering section of river, were used as a guide for extrapolating future morphology conditions in sub-reach 3; specifically, channel width and period of meander bends from sub-reach 2 were extrapolated to sub-reach 3. The July 1999 cross section data were physically modified to reflect the dominant morphology features in sub-reach 2: 1) the sand layer was removed to the depth of the current gravel deposits; 2) a meandering channel pattern was incorporated; and 3) the channel width was decreased to approximately 250 ft. Channel characteristics for these modified cross sections were estimated using the HEC-RAS model and then averaged. With the emerging gravel bed and a change in channel pattern to meandering, physical channel attributes are expected to change dramatically: channel width will decrease by at least half, while doubling the channel depth. Although the bed slope is expected to decrease (due to the increased channel length of the meandering channel), the water velocity is still expected to increase due to the reduced channel area as predicted in the SAM results.

Table 21: Average future conditions for sub-reach 3, based on a slightly meandering, gravel bedded channel, San Acacia Reach.

	Width (ft)	Depth (ft)	Area (ft ²)	Velocity (ft/sec)	Mean Bed Slope (ft/ft)
Current Conditions	640	2.5	1600	3.7	0.00092
Future Estimated Conditions	250	5.0	1250	4.0	0.00082

Using the modified channel characteristics, a stable grain size analysis found that although the median gravel sizes currently found in sub-reach 3 are likely mobile, the channel armoring bed material (d_{84} sediment size) was not. Yang’s gravel sediment transport model

(1984) estimated the potential mobility of particle sizes found in the current gravel deposits in sub-reach 3. The channel forming flow of 5,000 cfs, and the estimated future channel characteristics (Table 21) were used in the analysis. The particle size most likely to form an armor layer, the d_{84} , is estimated to be approximately 40 mm (Table 20) in sub-reach 3, while the median particle size (d_{50}) was 16 mm. The sediment transport model indicated that the current median particle size is mobile; however, the current d_{84} particle size is not mobile. These data suggest that the channel forming flow will erode the sand layer and create an armored gravel layer. Since armor layers naturally impede bed erosion, the rate of degradation in this reach will likely decrease or even stop as the gravel layer is 're-worked' by high flows.

5.3.4 Future Conditions of Sub-Reach 4

Sub-reach 4, a straight, narrow, deep channel has not changed much since 1972 (Table 11), except in elevation, which is expected to stabilize in the near future. Moderately tall terraces confine the channel and sufficiently contain channel forming flows. The SAM model results indicate that channel width is stable; the channel bed contains little gravel. The one notable feature that is changing in this sub-reach is the area at the Arroyo de la Parida confluence. Due to a major channel modification prior to the 1960's, the arroyo flows through an abandoned reach of the Rio Grande before joining the current Rio Grande channel. Since the 1960's, the larger sediments (i.e., gravel) transported by the arroyo were deposited in the abandoned channel, and not in the current channel. However, in recent years (post 2000), the arroyo has filled in the abandoned channel and is now transporting its total load to the current Rio Grande channel. These arroyo sediments are now deposited in the Rio Grande, creating a sediment fan that extends across the river. The fan is composed mostly of gravel and cobble sized sediment, some of which is being transported downstream by the Rio Grande. The fan is approximately 3 feet taller than the former channel height measured in 1999. The fan is expected to persist long-term and is already creating a point of stable channel bed elevation in the Rio Grande. With a stable bed point, channel degradation upstream of the arroyo is expected to decrease or even stop.

Sediment sizes in this sub-reach are changing rapidly due to the supply of coarse material from Arroyo de la Parida. The sediment fan is creating two features in the Rio Grande: a backwater/pool upstream of the fan, and a gravel bed downstream of the fan. The extent of the upstream backwater area is presently unrealized; however, by extrapolating the current stable channel slope upstream of the confluence (Figure 27), the backwater affects of the fan may reach the sub-reach 3 boundary. In this 1.5 miles, the slope is decreased, and a modest amount of finer sediments are expected to be deposited and to be retained long-term. Downstream of the fan, the sediment size is expected to increase to at least gravel size. The development of a stable-channel elevation and the deposition of gravel in the lower section of the sub-reach are expected to hinder channel incision. Hence, degradation rates in sub-reach 4 are expected to decrease or even cease due to the re-connection of Arroyo de la Parida to the Rio Grande.

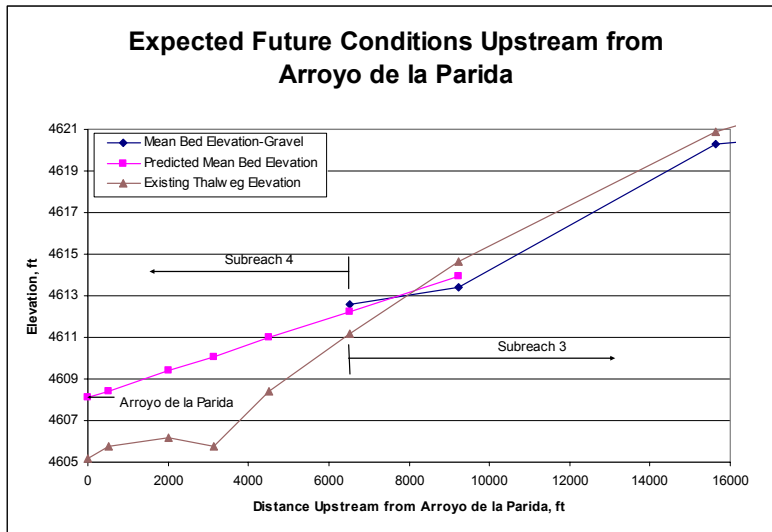


Figure 27: Future elevation conditions of Sub-Reach 4, Rio Grande – San Acacia Reach.

5.3.5 Potential Levee Breach Locations

Viewing current channel erosion patterns and extrapolating a meandering pattern throughout sub-reach 3, the constructed levee on the west side of the channel may become threatened in several locations. Currently, two locations have potential of threatening the levee: about 1 mile upstream and 1 mile downstream of Arroyo Alamillo (Figure 28). In both of these locations, migrating channel bends have already become established, and are migrating in the direction of the levee. With continued migration of the channel, these locations will threaten levee integrity. Downstream of these locations in sub-reach 3 (Transport Zone 7), approximately 2 miles of river bank/levee have been identified as potential sites of future erosion. As sub-reach 3 converts to a meandering pattern (with a similar periodicity of meandering as found upstream), approximately 3 locations in this 2 mile section may threaten the levee. Since the distance between the current channel and the levee is short in this section, the levee threat may begin shortly after the channel pattern has evolved to meandering. With the change in channel pattern to a meandering channel pattern, the threat of levee erosion increases significantly from the less erosive braided channel pattern.

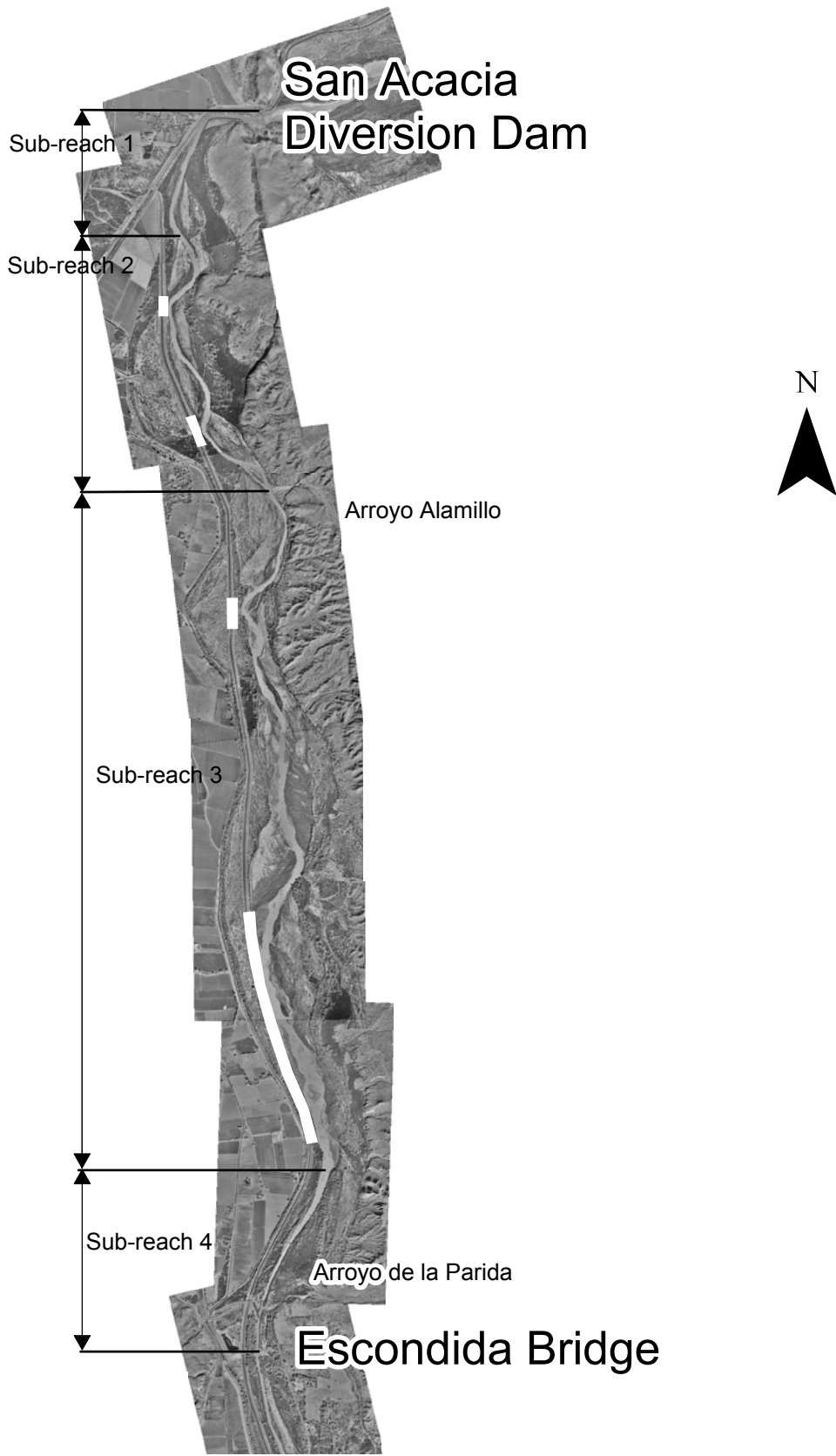


Figure 28: Three USBR river maintenance priority sites with levee erosion concerns, plus one site of estimated future levee erosion (the downstream most highlighted section), Rio Grande; San Acacia Reach.

5.3.5 Summary of Future Conditions

The Rio Grande in the San Acacia Reach has undergone several major geomorphic changes in the recent past, however the evolution is not complete; future conditions analysis indicates that channel pattern changes will continue, the emergence of a gravel bed will extend downstream of its present location, and that with these changes, channel elevation may become more stable. Channel pattern is stable in sub-reach 1 due mostly to its high confinement. However, sub-reaches 2 and the upstream portion of 3 have recently converted to a slightly meandering channel pattern. The remainder of sub-reach 3 appears to be preparing to convert to a single-threaded meandering channel, which will be the most dramatic change to the current channel features present in the reach. Channel pattern in sub-reach 4 appears stable, as in sub-reach 1. The emergence of a gravel bed, which began in the late 1980's at the diversion dam has migrated about 4 miles downstream (upstream portion of sub-reach 3) and is expected to connect with the Arroyo de la Parida fan in the future. As a result of Arroyo de la Parida reconnecting to the Rio Grande and the emergence of a protective gravel layer throughout the whole reach, the rate of degradation is expected to subside if not cease altogether.

6.0 CONCLUSIONS

- Suspended sediment (sand load) has dropped by 80% since 1978 at the San Acacia gaging station.
- The channel was straight prior to channelization efforts in the 1950's, and continues to be mostly straight.
- Active channel width has decreased from an average of 1700 feet in 1918 to 460 feet in 1999.
- The channel bed has decreased in elevation approximately 13 feet near the dam, and 8 feet near Escondida Bridge.
- Two periods of degradation have been identified by analyzing terrace formation and survey data: 1918-1949 and 1985-1995. A series of distinct terraces define these periods of incision.
- Although the channel bed was historically sand bedded, bed samples dating back to 1988 indicate that the channel bed is converting to gravel.
- At present, much of the channel bed consists of a bi-modal sediment distribution: a 2-3 feet thick sand layer overlying a distinct layer of gravel.
- The dominant source of gravel sized sediment is arroyos.
- Gravel sized sediment, rather than the sand, appears to be quasi-stable at the current bed slopes.
- Sediment transport models indicate that within days, an average spring runoff can excavate the current deposits of sand found in the first 4 miles downstream of the dam.
- The channel pattern/morphology is changing: a meandering channel pattern has formed in the first third of the reach, and appears to be emerging in the remainder of the reach.
- The currently wide section of this reach (sub-reach 3) has begun to form a solid gravel layer beneath the sand, and appears to be converting to a meandering channel pattern.
- Arroyo de la Parida in sub-reach 4, is supplying gravel to the Rio Grande and creating a stable elevation point that is expected to stabilize incision.
- Channel pattern change in sub-reach 3 increases the threat of river erosion on the west levee.

7.0 LITERATURE CITED

- Biedenharn, D. S., Little, C. D., and Thorne, C. R., 1987, Magnitude and Frequency Analysis of Large Rivers, in Ragan, R. M. (Ed.), Hydraulic Engineering, Proceedings of the National Conference on Hydraulic Engineering, American Society of Civil Engineers, Williamsburg, p. 782-787.
- Brown, L. D., Krumhansl, P. A., Chapin, C. E., Sanford, A. R., Cook, F. A., Kaufman, S., Oliver, J. E., and Schilt, F. S., 1979, COCORP seismic reflection studies of the Rio Grande rift, in Rieker, R. E., ed., Rio Grande rift: Tectonics and magmatism: Washington, D. C., American Geophysical Union, p. 169-184.
- Chapin, C. E., 1988, Axial basins of the northern and central Rio Grande rifts; in Sloss, L. L., ed., Sedimentary cover-North American Craton: U.S.: Geological Society of America DNAG Volume D-2, Boulder, pp. 165-170.
- Colby, B. R., and Hembree, C. H., 1955, Computation of Total Sediment Discharge, Niobarra River, near Cody, Nebraska, Geological Survey Water-Supply Paper 1357, Government Printing Office, Washington, D.C., 187 p.
- Graf, W. L., 1994, Plutonium and the Rio Grande, Environmental Change and Contamination in the Nuclear Age, Oxford University Press, New York.
- Hawley, J. W., 1978, Guidebook to Rio Grande rift in New Mexico and Colorado, New Mexico Bureau Mines & Mineral Resources, Circular 163, 241p+.
- Hey, R. D., 1975, Design discharge for natural channels, in Hey, R. D., and Davies, T. D. (Eds.), Science, Technology and Environmental Management, Saxon House, p. 73-88.
- Hydrosphere, 2000, compiled climate data from the National Climate Data Center, 1993-2000 Hydrosphere Data Products, Inc., Hydrodata for Windows, Version 4.00.
- Julien, P. Y., 1995, Erosion and Sedimentation, Cambridge University Press, New York, NY, pp. 185-187.
- Klumpp, C. C., 1992, User's Manual for STARCAL, a Root Mean Square Error Computer Program, U.S. Bureau of Reclamation, Sedimentation Section, Denver, CO, 59 p.
- Knighton, David, 1998, Fluvial Forms and Processes, a New Perspective, Arnold Publishers, London, Great Britain 383 p.
- Lagasse, P. F., 1980, An Assessment of the Response of the Rio Grande to Dam Construction-Cochiti to Isleta, U. S., Army Corps of Engineers Technical Report, Albuquerque, New Mexico, 133 p.

- Lane, E. W., 1957, Design of Stable Channels, Transactions, American Society of Civil Engineers, Vol. 120.
- Larsen, S., and Reilinger, R., 1983, Recent Measurements of Crustal Deformation Related to the Socorro Magma Body, New Mexico, in New Mexico Geological Society Guidebook, 34th Field Conference, p. 119-121.
- Leopold, L. B., 1994, A View of the River, Cambridge, MA: Harvard University Press, 298 p.
- Leopold, L. B., Wolman, M. G., and Miller, J. P., 1964, Fluvial processes in geomorphology, San Francisco, W. H. Freeman, 522 p.
- Meyer-Peter, E., and Muller, R., 1948, Formulas for Bed-Load Transport, International Association for Hydraulic Structures, Second Meeting, Stockholm, Sweden.
- Morgan, P., Seager, W. R., and Golombek, M. P., 1986, Cenozoic Thermal, Mechanical and Tectonic Evolution of the Rio Grande Rift, Journal of Geophysical Research, Vol. 91, No. B6, pp. 6263-6276.
- Orvis, C. J., and Randle, T. J., 1987, STARS: Sediment Transport and River Simulation Model, U.S. Bureau of Reclamation, Engineering and Research Center, Denver, CO, 212 p.
- Ouchi, S., 1983, Response of Alluvial Rivers to Active Tectonics, Ph.d. dissertation, Earth Resources Department, Colorado State University, Fort Collins, Colorado, 205 p..
- Sanford, A. R., Alptekin, O. S., and Topozada, T. R., 1973, Use of Reflection Phases on Microearthquake Seismograms to Map an Unusual Discontinuity Beneath the Rio Grande rift, Seismological Society of America Bulletin, v. 63, p. 2031-2034.
- Sanford, A. R., Mott, R. P., Jr., Shuleski, P. J., Rinehart, E. J., Caravella, F. J., Ward, R. M., and Wallace, T. C., 1977, Geophysical Evidence for a Magma Body in the Crust in the Vicinity of Socorro, New Mexico, in Heacock, J. E., ed., The Earth's crust: American Geophysical Union Geophysical Monograph 20, p. 385-403.
- Schoklitsch, 1932, Prevention of Scour and Energy Dissipation, Translated by E. F. Wilsey, U. S., Bureau of Reclamation.
- Shields, A., 1936, Anwendung der Ähnlichkeitsmechanik und der Turbulenzforschung auf die Geschiebebewegung, Translated by W. P. Ott and J. C. Van Uchelen, California Institute of Technology, Pasadena, California, 26 p.
- Strand, R. I., and Pemberton, E. L., 1982, Reservoir Sedimentation, Technical Guideline for Bureau of Reclamation.

- Rosgen (1996), Applied River Morphology, Wildland Hydrology, Pagosa Springs, Colorado, 360+ p.
- U.S. Army Corps of Engineers, 1998, Hydrologic Engineering Center-River Analysis System User's Manual, Version 2.2, Hydrologic Engineering Center, Davis, California, 227+ p.
- U.S. Army Corps of Engineers, 1998, SAM-Hydraulic Design Package for Channels User's Manual, Waterways Experiment Station, Vicksburg, Mississippi, 144+ p.
- U.S. Bureau of Reclamation, 1969, Guide for Application of Total Sediment Load Computer Program, Sedimentation Branch, Division of Project Investigations, Office of Chief Engineer, Denver, Colorado, 9 p.
- U.S. Bureau of Reclamation, 1995, Scour and Fill, version 7.1.
- U.S. Bureau of Reclamation, 2000, Southwest willow flycatcher survey, unpublished data.
- U.S. Bureau of Reclamation and U.S. Army Corps of Engineers, October, 1999, Programmatic Biological Assessment of Federal Discretionary Actions Related to Water Management on the Middle Rio Grande, New Mexico, 223+ p.
- U.S. Geological Survey, 1895-2000, Surface Water Records, Water Resources Data, New Mexico.
- Yang C. T., 1972, Unit Stream Power and Sediment Transport, Journal of the Hydraulics Division, ASCE, vol. 18, no. HY 10, Proceeding Paper 9295, pp. 1805-182.
- Yang C. T., 1984, Unit Stream Power Equation for Gravel, Journal of Hydraulic Engineering, ASCE, vol. 110, no. 12.
- Wolman, M. G., and Leopold, L. B., 1957, River flood plains: some observations on their formation: U.S., Geological Survey Professional Paper 282-C, p. 87-107.
- Wolman, M. G., and Miller, J. P., 1960, Magnitude and frequency of forces of geomorphic processes, Journal of Geology, v.68, p. 54-74.